Reprogramming of cardiac phosphoproteome, proteome and transcriptome confers resilience to chronic adenylyl cyclase-driven stress

Jia-Hua Qu[1,2], Khalid Chakir[1], Kirill V. Tarasov[1], Daniel R. Riordon[1], Maria Grazia Perino[1], Allwin Jennifa Silvester[1], and Edward G. Lakatta[1]*

1. Laboratory of Cardiovascular Science, Intramural Research Program, National Institute on Aging, National Institutes of Health, Baltimore, MD 21224, USA.
2. Department of Immunology, St. Jude Children's Research Hospital, Memphis, TN 38105, USA

Address correspondence to:

Dr. Edward G. Lakatta*

Laboratory of Cardiovascular Science

Intramural Research Program

National Institute on Aging

National Institutes of Health

251 Bayview Boulevard

Suite 100

Baltimore, MD 21224

USA.

Tel: +1 410-558-8202

lakattae@grc.nia.nih.gov

Abstract

Our prior study (Tarasov, K. V. et al., 2022) discovered that numerous adaptive mechanisms emerge in response to cardiac-specific overexpression of adenylyl cyclase type 8 (TGAC8) which included overexpression of a large number of proteins. Here we conducted an unbiased phosphoproteomics analysis in order to determine the role of altered protein phosphorylation in the adaptive heart performance and protection profile of adult TGAC8 left ventricle (LV) at 3-4 months of age, and integrated the phosphoproteome with transcriptome and proteome. Based on differentially regulated phosphoproteins by genotype, numerous stress-response pathways within reprogrammed TGAC8 LV, including PKA, PI3K and AMPK signaling pathways, predicted upstream regulators (e.g., PDPK1, PAK1 and PTK2B), and downstream functions (e.g., cell viability, protein quality control), and metabolism were enriched. In addition to PKA, numerous other kinases and phosphatases were hyper-phosphorylated in TGAC8 vs. WT. Hyper-phosphorylated transcriptional factors in TGAC8 were associated with increased mRNA transcription, immune responses and metabolic pathways. Combination of the phosphoproteome with its proteome and with the previously published TGAC8 transcriptome enabled the elucidation of cardiac performance and adaptive protection profiles coordinately regulated at post-translational modification (PTM) (phosphorylation), translational and transcriptional levels. Many stress-response signaling pathways, i.e., PI3K/AKT, ERK/MAPK and ubiquitin labeling, were consistently enriched and activated in the TGAC8 LV at transcriptional, translational and PTM levels. Thus, reprogramming of the cardiac phosphoproteome, proteome and transcriptome confers resilience to chronic adenylyl cyclase-driven stress. We identified numerous pathways/function predictions via gene sets, phosphopeptides, and phosphoproteins, which may

point to potential novel therapeutic targets to enhance heart adaptivity, maintaining heart performance while avoiding cardiac dysfunction.

Keywords

left ventricle, adenylyl cyclase 8, AC-cAMP-PKA-Ca^{2+} signaling, phosphoproteome, proteome, transcriptome, PI3K/AKT signaling pathway

Introduction

Cardiac-specific overexpression of AC8 (TGAC8) markedly increases the heart rate and ejection fraction, similar to acute exercise but chronic and in the absence of corporal exertion, which persists on a 24 hours per day and 7 days per week basis[1-4]. Despite this constant high-level of heart performance driven by markedly elevated level of AC8-cAMP-PKA-Ca^{2+} signaling, which typically proceeds to near-term cardiac dysfunction, the TGAC8 survives for an extended period of time, up to about one year of age without excessive mortality[5]. Adaptive mechanisms that emerge in the TGAC8 heart confer resilience to this marked chronic stress of increased AC8-cAMP-PKA-Ca^{2+} signaling and include the enrichment and activation of a large number of proteins involved in multiple signaling pathways related to nutrient sensing, energy production, growth factor signaling, and cell proliferation[5].

As the body is a complex system, multiple levels of coordinated regulatory mechanisms are requisite to defend against stimuli and maintain health[6-9]. Phosphorylation is one of the most important and has been the most extensively studied post-translational modifications (PTM) of proteins. Various kinases and phosphatases within cells phosphorylate and dephosphorylate, respectively, a myriad of proteins to regulate their activities and affect multiple signaling

67 pathways. Because the PKA signaling pathway was highly enriched in TGAC8 vs. WT[5], we
68 reasoned that protein phosphorylation differed between TGAC8 and WT, and protein
69 phosphorylation modification plays a crucial role in the remarkable adaptative capacity of the
70 TGAC8 heart in response to markedly increased AC8-cAMP-PKA-Ca^{2+} signaling.

71 By the utilization of TMT-labeling mass spectrometry (MS), we identified 12963
72 phosphopeptides and 3646 phosphoproteins, and observed a general upregulation of
73 phosphorylation. By comparing genotypic differences in the proteome and phosphoproteome of
74 the present study with genotypic differences in the transcriptome published previously[5], we
75 sought to determine whether some adaptive mechanisms that emerge in the TGAC8 left ventricle
76 (LV) are regulated at transcriptional, translational and PTM (phosphorylation) levels. We
77 observed enrichments of phosphorylation, upregulation of kinase expression, and predicted
78 activation of upstream kinases to expand our understanding of the regulatory mechanisms the
79 TGAC8 utilizes to adapt to the chronic stress of activated AC8-cAMP-PKA-Ca^{2+} signaling. We
80 integrated genotypic difference between the TGAC8 and WT of the phosphoproteome with the
81 transcriptome and proteome, which broadened our understanding how changes in the
82 transcription, translation and PTM of proteins in the TGAC8 LV may singly or coordinately
83 enable the TGAC8 to endure the chronic AC8-induced stress.

84

85 **Materials and Methods**

86 **1. Animals**.

87 The cardiac-specific overexpression of AC8 (TGAC8) mouse, generated by inserting a cDNA
88 coding for human AC8 after the murine α-myosin heavy chain promoter, was a gift from Nicole

Defer/Jacques Hanoune, Unite de Recherches, INSERM U-99, Hôpital Henri Mondor, F-94010 Créteil, France. The three-month old male TGAC mice were used as study cases, and age matched WT littermates, in the C57/BL6 background, were used as controls. All studies were performed in accordance with the Guide for the Care and Use of Laboratory Animals published by the National Institutes of Health (NIH Publication no. 85-23, revised 1996). The experimental protocols were approved by the Animal Care and Use Committee of the National Institutes of Health (protocol #441-LCS-2016).

2. Isolate and store mouse heart.

Three-month old male C57 mice (TGAC8 and WT) were euthanized, and the heart was isolated. The left ventricle (LV) tissues were extracted and stored in tubes at -80°C.

3. Mass spectrometry for phosphoproteome and data process.

TGAC8 and WT LVs were sent to National Heart, Lung, and Blood Institute, National Institutes of Health, Bethesda to conduct mass spectrometry (MS) using the standard tandem mass tag (TMT) labeling method to obtain the phosphoproteome and total proteome concurrently in the same platform. Mass spectrometry manipulation referred to our recently published paper[5].

Proteins from each group of samples are being quantified using the Bradford Assay Kit. Two-hundred micrograms of protein from each group will be labeled with Amine-Reactive Tandem Mass Tag Reagents (TMT Label Reagents; Thermo Scientific) according to the protocol supplied by the manufacturer. Briefly, protein will be denatured followed by reduction (TCEP) and

110 alkylation (iodoacetamide) and then the alkylated proteins (200ug) for each sample were
111 precipitated in 6 volumes of ice-cold acetone at -20 °C overnight and later reconstituted in
112 Triethylammonium bicarbonate. Each sample was digested overnight using Trypsin enzyme
113 (enzyme to substrate ratio of 1:12.5) to get the peptide solution. Trypsin will cleave proteins at
114 lysine and arginine amino acid residues yielding tryptic peptides.

115 The 10-plex tandem mass tag (TMT) labeling was carried out according to Thermo Fisher
116 Scientific's TMT Mass Tagging kits protocol. Each of the TMT 10-plex label reagents were
117 reconstituted in Acetonitrile (ACN) and digested peptides from each sample were incubated with
118 specific tags (126, 127N, 127C, 128N, 128C, 129N, 129C, 130N,130C and 131 respectively) for
119 about 1 hour at room temperature. The TMT labeled samples are then combined and fractionated
120 using Off-Line high pH Basic Reverse Phase Fractionation to decrease the complexity of the
121 sample and to increase the number of peptides being identified into a total of 24 fractions which
122 will be later analyzed using LC-MS/MS. About 5% of the labeled tryptic peptides from each of
123 24-fractions were used for global proteomics analysis by nanoLC-MS/MS analysis while the
124 remaining 95% of samples in the 24-fractions were subjected to subsequent TiO2-enrichment for
125 quantitative phosphoproteomics analysis.

126 TiO2 enrichment was conducted using a Titansphere Phos-kit (GL biosciences Inc.). The TMT
127 10-plex tagged tryptic peptides were reconstituted in Buffer B (25% lactic acid in 1% TFA, 80%
128 Acetonitrile). The TiO2 SpinTip (1mg resin/10ul tip) was incubated with the sample, washed
129 using the wash buffer following manufacturers protocol and the phosphopeptides were eluted in
130 elution buffer sequentially using 5% ammonium hydroxide solution and 5% pyrrolidine solution.
131 The eluted fraction was dried and reconstituted in 0.1% FA for subsequent clean-up using the

132 ZipTip C18-tips (Millipore). The sample from elution fraction of C18-tips were dried and
133 reconstituted in 0.1%FA for LC-MS/MS analysis.

134 The flow-through fraction and the wash fraction from the TiO2 spinTip was collected, pooled
135 into a total of 6 fractions and speedvac dried which will be later used for Fe-IMAC
136 phosphoenrichment protocol. The peptide sample from 6-pooled flow-through fractions from
137 TiO2 enrichment underwent second round of phosphoenrichment using High-Select Fe-NTA
138 Phosphopeptide Enrichment Kit (Thermo Scientific). The eluted fraction was dried and
139 reconstituted in 0.1% FA for subsequent LC-MS/MS analysis.

140 Protein identification by LC-MS/MS analysis of peptides was performed using an Orbitrap
141 Fusion Lumos Tribid mass spectrometer (Thermo Fisher Scientific, San Jose, CA) interfaced
142 with an Ultimate 3000 Nano-HPLC apparatus (Thermo Fisher Scientific, San Jose, CA).
143 Peptides were fractionated by EASY-Spray PepMAP RPLC C18 column (2µm, 100A, 75 µm x
144 50cm) using a 120-min linear gradient of 5-35% ACN in 0.1% FA at a flow rate of 300 nl/min.
145 The instrument was operated in data-dependent acquisition mode (DDA) using FT mass analyzer
146 for one survey MS scan on selecting precursor ions followed by top 3 second data-dependent
147 HCD-MS/MS scans for precursor peptides with 2-7 charged ions above a threshold ion count of
148 10,000 with normalized collision energy of 37%. Survey scans of peptide precursors from 300 to
149 2000 m/z were performed at 120k resolution and MS/MS scans were acquired at 50,000
150 resolution with a mass range m/z 100-2000.

151 All MS and MS/MS raw spectra of TMT experiments from each set were processed and searched
152 using Sequest HT algorithm within the Proteome Discoverer 2.2 (PD2.2 software, Thermo Fisher
153 Scientific).The settings for precursor mass tolerance was set at 12 ppm, fragment ion mass
154 tolerance to 0.05 Da, trypsin enzyme with 2 mis cleavages with carbamidomethylation of

155 cysteine, TMT6-plex (lysine), TMT6-plex (peptide N-term) as fixed modification and
156 deamidation of glutamine and asparagine, oxidation of methionine as variable modifications.
157 The mouse sequence database from Swiss sprot was used for database search. Identified peptides
158 were filtered for maximum 1% FDR using the Percolator algorithm in PD 2.2 along with
159 additional peptide confidence set to high. Only peptide spectra containing all reporter ions were
160 designated as "quantifiable spectra" and used for peptide/protein quantitation. The final lists of
161 protein identification/quantitation were grouped and further filtered by PD 2.2 with at least 2
162 unique peptides per protein identified with high confidence. The quantitative protein ratios were
163 weighted and normalized by the median ratio for all quantifiable spectra of the peptides
164 pertaining to total protein identified.

165 For quantitative phosphopeptides analysis, an additional phosphorylation on Ser, Thr, Tyr
166 residues were specified as variable modifications. To confidently localize phosphorylation sites,
167 the phosphoRS 3.0 node integrated in PD 2.2 workflow was used. The algorithm of phosphoRS
168 3.0 software enables automated and confident localization of phosphosites by determining
169 individual probability values for each putatively phosphorylated site within the validated peptide
170 sequences. For each relative ratio group of phosphopeptides/sites, no normalization was applied.

171 To remove low quality signal, we remained peptides tagged with the medium and high
172 confidence. We divided the expressions of phosphoproteins to those of total proteins to obtain
173 the normalized phosphoproteome. As the expressions appeared to be near normal distribution,
174 we calculated the fold change by dividing the average value of TGAC8 samples by the average
175 value of WT samples, and calculated p-value using two-sided unpaired Student's t-test. Data
176 were deposited in MassIVE (ID: MSV000089850).

177

178 **4. Analyses of the TGAC8 LV transcriptome.**

179 The processed transcriptomic data were obtained from our recently published work (GEO:
180 GSE205234)[5]. The significantly changed mRNAs (TGAC8 vs. WT, q-value < 0.05) were
181 uploaded into DAVID[2] (version: 6.8; https://david.ncifcrf.gov/home.jsp) for Gene Ontology
182 (GO) term enrichments, and were also imported into Ingenuity Pathway Analysis[3] (IPA
183 (QIAGEN, March 2020)) for upstream kinases and phosphatases prediction. Kinases and
184 phosphatases were selected from the transcriptome and their changes at mRNA level were
185 displayed to observe their regulation by the overexpression of AC8.

186

187 **5. Analyses of phosphoproteome and proteome.**

188 Both unnormalized and normalized phosphoproteome were analyzed and visualized in PCA,
189 heatmap, and volcano plots. With the cutoff -log(p-value) > 1.3 and absolute(log2(fold change))
190 ≥ 0.4, we obtained the significantly changed unnormalized and normalized phosphoproteins
191 (TGAC8 vs. WT) and imported them into IPA for functional analyses respectively, and
192 compared the canonical pathway enrichments from these two datasets. In IPA, the upstream
193 kinases were predicted based upon the unnormalized phosphoproteom, and the regulatory
194 pathways from the predicted upstream kinases to downstream effective signaling pathways were
195 generated. Molecular and cellular functions were also enriched in IPA. The similar analyses to
196 those conducted in the TGAC8 LV transcriptome were also done in the TGAC8 LV total
197 proteome to observe the GO term enrichment, predicted activities of upstream kinases and
198 phosphatases, and expression of kinases and phosphatases at protein level.

199

200 **6. Analyses of phosphopeptides.**

201 The upregulated phosphopeptides (TGAC8 vs. WT, p-value < 0.05 and log2(fold change) > 0)
202 were processed in R. After split of peptides with multiple phosphosites into individual peptides
203 and filtering of ambiguously identified sites, 2264 phosphopeptides were selected. Protein
204 peptide sequences of full length were downloaded from Uniprot database[10] and matched to the
205 protein accessions corresponding to processed and selected phosphopeptides. Peptides centered
206 on the phosphosites and flanked by 6 amino acids on the N and C termini respectively were
207 extracted from the matched protein peptide sequences, and uploaded into WebLogo[11]
208 (http://weblogo.threeplusone.com/) and iceLogo[12] (https://iomics.ugent.be/icelogoserver/) for
209 sequence motif analysis. In WebLogo online analysis, different amino acids were labeled in
210 different colors representing different chemical properties (refer to figure legend). In iceLogo
211 online analysis, a public amphiphilicity index of polar amino acids reported by Mitaku and
212 colleagues[13] was used as an aid to characterize the amino acid preference at membrane-water
213 interfaces. In addition, the phosphopeptides of PI3K/AKT substates were summarized and
214 displayed in stacked bar plot.

215

216 **7. Integrative analyses of transcriptome, proteome and phosphoproteome.**

217 The changes of significantly regulated molecules (TGAC8 vs. WT, q-value or p-value < 0.05) in
218 transcriptome, total proteome, and unnormalized phosphoproteome were displayed in circos plot.
219 In addition, the changes at different level were compared and visualized in correlation scatter
220 plots. The discordant proteins whose change directions in total proteome and phosphoproteome

221 were opposite were used to analyze the specific regulation at the phosphorylation level by the
222 use of Reactome and GO (Cellular Component and Biological Process) databases.

223 As to the coordinated regulation, the above mentioned significantly regulated molecules
224 (TGAC8 vs. WT) in each dataset were imported into IPA for canonical pathway enrichment.
225 PI3K/AKT, ERK/MAPK and protein ubiquitination signaling pathways were coordinated across
226 all omics. The phosphopeptides of protein substrates of PI3K were extracted from the
227 phosphopeptide dataset and the numbers of changed phosphopeptides (TGAC8 vs. WT) were
228 summarized and visualized in stacked bar plot. The PI3K/AKT signaling pathway were
229 visualized in IPA, and nodes in the pathways were marked in different colors in terms of their
230 changes at different levels.

231 As kinases and phosphatases are pivotal in phosphorylation, and transcription factors (TFs) are
232 important in transcription regulation, they were extracted from transcriptome, proteome, and
233 phosphoproteome to observe their changes (TGAC8 vs. WT) and deduce their role in the
234 reprogram of phosphoproteome. The upstream transcription regulators including but not only
235 TFs were predicted on the basis of transcriptome and proteome by the utilization of knowledge
236 base in IPA, and their expressions were searched in multiple datasets. Furtherly, TFs that were
237 significantly regulated at phosphorylation level (TGAC8 vs. WT, $p\text{-value} < 0.05$) were defined
238 as significantly changed phosphorylated TFs in this research, and they were uploaded into
239 STRING database[4] (version: 11.0; http://string-db.org/) to generate protein-protein interaction
240 network and enrich KEGG pathways. They were also imported into IPA for canonical pathway,
241 molecular and cellular functions enrichments.

242

243 **8. Western blot.**

244 Snap-frozen left ventricle (LV) tissue from three-month-old male mice was homogenized and
245 lysed in ice cold RIPA buffer (Thermo Fisher Scientific: 25 mM Tris-HCl (pH 7.6), 150 mM
246 NaCl, 1% NP-40, 1% sodium deoxycholate, 0.1% SDS) supplemented with a Halt protease
247 inhibitor cocktail (Thermo Fisher Scientific), Halt phosphatase inhibitor cocktail (Thermo Fisher
248 Scientific) and 1 mM phenylmethyl sulfonyl fluoride, using a Precellys homogenizer (Bertin
249 Instruments) with tissue homogenization kit CKMix (Bertin Instruments) at 4 °C. Extracts were
250 then centrifuged at 10,000×g for 10 min at 4 °C and the protein concentration of the soluble
251 fraction determined using the Bicinchoninic Acid (BCA) Assay (Thermo Fisher Scientific).
252 Samples were denatured in Laemmli sample buffer (BioRad Laboratories) containing 355 mM 2-
253 mercaptoethanol at 95 °C for 5 min, and proteins (10–50 μg/lane) resolved on 4–20% Criterion
254 TGX Stain Free gels (Bio-Rad Laboratories) by SDS/PAGE. Gels then exposed to UV
255 transillumination for 2.5 min to induce crosslinking of Stain Free gel trihalo compound with
256 protein tryptophan residues. Proteins were then transferred to low fluorescence polyvinylidene
257 difluoride (LF-PVDF) membranes (BioRad Laboratories) using an electrophoretic transfer cell
258 (Mini Trans-Blot, Bio-Rad). Membrane total protein was visualized using an Amersham Imager
259 600 (AI600) (GE Healthcare Life Sciences) with UV transillumination to induce and a capture
260 fluorescence signal.

261 Blocked membranes (5% milk/tris-buffered saline with Tween-20, TBST) were incubated with
262 the following primary antibodies: (1) Anti-Phospho-PKA Substrate (RRXS*/T*) antibody, Cell
263 Signaling Technologies, Cat.#9624, 1:1000 dilution; (2) Anti-Ubiquitin antibody produced in
264 rabbit, Sigma-Aldrich, SAB1306582, 1:200 dilution; (3) Anti-pan-AKT antibody, Cell Signaling
265 Technologies, Cat.#4691, 1:1000 dilution; (4) Anti-Phospho-pan-AKT (Thr308) antibody, Cell

266 Signaling Technologies, Cat.#13038, 1:1000 dilution; (5) Anti-Phospho-pan-AKT (Ser473)
267 antibody, Cell Signaling Technologies, Cat.#4060, 1:1000 dilution; (6) Anti-AKT2 antibody,
268 Abcam, Cat.#13038, 1:1000 dilution; (7) Anti-Phospho-AKT2 (Ser473) antibody, Cell Signaling
269 Technologies, Cat.#ab131168, 1:1000 dilution; (8) Anti-ERK1/2 antibody, Cell Signaling
270 Technologies, Cat.#4695, 1:1000 dilution; (9) Anti-Phospho-ERK1/2 (Thr202/Tyr204) antibody,
271 Cell Signaling Technologies, Cat.#4376, 1:1000 dilution; (10) Anti-p21 Ras antibody, Cell
272 Signaling Technologies, Cat.#3965, 1:1000 dilution; (11) Anti-GAPDH antibody, Santa Cruz
273 Biotechnology, Cat.# sc-32233, 1:1000 dilution; (12) Anti-c-Raf antibody, ThermoFisher
274 Scientific, Cat.# PA5-29333, 1:1000 dilution; (13) Anti-Phospho-c-Raf (Ser338) antibody, Cell
275 Signaling Technology, Cat.# 9427, 1:1000 dilution; (14) Anti-MEK1/2 antibody, Cell Signaling
276 Technology, Cat.# 9126, 1:1000 dilution; (15) Anti-Phospho-MEK1/2 (Ser221) antibody, Cell
277 Signaling Technology, Cat.# 2338, 1:1000 dilution.

278 Primary antibodies were then detected using horseradish peroxidase (HRP) conjugated antibody
279 (Invitrogen) at 1:10,000. Bands were visualized using Pierce SuperSignal West Pico Plus ECL
280 substrate kits (Thermo Scientific), the signal captured using an Amersham Imager 600 (AI600)
281 (GE Healthcare Life Sciences) and quantified using ImageQuant TL software (GE Healthcare
282 Life Sciences). Band density was normalized to total protein. Two-tailed unpaired Student's t
283 test with Welch's correction was used for statistics.

284

285 **9. Protein synthesis detection.**

286 Protein synthesis was assessed by SUnSET-Western Blot as previously described in the above
287 section. Briefly, the puromycin solution was prepared in PBS, sterilized by filtration, and a

288 volume of 200 µl was injected in mice intraperitoneally, to achieve a final concentration of 0.04
289 µmol/g of body mass. After 30 min, mice were sacrificed, the LV was harvested and snap frozen
290 in liquid nitrogen. Protein extraction was performed using Precellys, quantified with BCA assay
291 25 µg of total protein were separated by SDS-PAGE; proteins were then transferred onto PVDF
292 membrane and incubated overnight in the anti-puromycin primary antibody (MABE343, Sigma-
293 Aldrich, St. Louis, MO). Visualization of puromycin-labeled bands were obtained using
294 horseradish peroxidase conjugated anti-mouse IgG Fc secondary antibody (Jackson
295 ImmunoResearch Laboratories Inc, West Grove, PA, USA), using Pierce Super Signal ECL
296 substrate kit (Pierce/ Thermo Scientific Rockford, IL). Chemiluminescence was captured with
297 the Imager AI600 and densitometry analysis was performed using ImageQuantTL software (both
298 by GE, Boston, MA). Total protein was used as control for protein loading. Genotypic
299 differences of protein synthesis were tested via an as unpaired t-test.

300

301 **10. Proteasome activity detection.**

302 Flash frozen tissue was homogenized in ice-cold cytosolic extraction buffer (50 mM Tris-HCl
303 pH 7.5, 250 mM Sucrose, 5 mM MgCl2, 0.5 mM EDTA, and 1 mM DTT). A bicinchoninic acid
304 (BCA) assay (Pierce) was used to determine the protein concentrations. All samples were equally
305 concentrated in proteasome assay buffer (50 mM Tris-HCl pH 7.5, 40 mM KCl, 5 mM MgCl2,
306 and 1 mM DTT). Proteasome activity was determined in the presence of 28 µM ATP using the
307 Suc-LLVY-AMC (18 µM, Boston Biochem #S280) fluorogenic substrate with and without
308 proteasome inhibition (MG 132, 1 mM, Sigma). The plate was read at an excitation wavelength
309 of 380 nm and an emission wavelength of 469 nm using a Spectramax M5 (Molecular Devices).

310 Activity was calculated by subtracting the background (proteasome inhibited value) from the
311 reading (proteasome activated value).

312

313 **11. Protein soluble and insoluble fractions detection.**

314 Protein aggregates were measured using Proteostat (Enzo, ENZ-51023) following the
315 manufacturer's instructions. For this assay left ventricle myocardial lysate (Cell Signaling lysis
316 buffer) was obtained, protein concentration assayed (BCA assay [Pierce]). Ten µg of protein
317 loaded into a 96-well microplate and protein aggregates were analyzed using the Proteostat assay
318 kit (Enzo Life Sciences) following the manufacturer's instructions. Background readings were
319 subtracted from sample recordings and were normalized to wild-type values.

320

321 **12. Data process and graphics production.**

322 Most raw data were precleared and processed using RStudio (version: 1.1.463) in R language
323 (version: 3.5.3), in which the tidyr package and dplyr package were applied. In addition,
324 GraphPad Prism (version: 7), Microsoft Excel (version: 2019) and Adobe Illustrator (version:
325 CC 2019) were also used for statistics and graphics. Venn diagrams were generated in Venny[5]
326 (version: 2.1.0; http://bioinfogp.cnb.csic.es/tools/venny/index.html). Circos plot was generated
327 using Circos software[6] in Perl language.

328

329 **Results**

330 **1. The TGAC8 reprograms the LV phosphoproteome.**

331 The TMT-labeling quantitative mass spectrometry (MS) identified **12963 phospho-peptides**
332 (File 1: Sheet 1) and **3646 phosphoproteins** (File 1: Sheet 2). The principal component analysis
333 (PCA) (Figure 1A) of the 3646 phosphoproteins in each mouse showed that the TG and WT
334 samples were distinguished into two groups completely. The heatmap (Figure 1B) showed the
335 intra-group consistency of upregulated phosphoproteins in TGAC8 compared to WT. Within the
336 cutoff at -log10(p-value) > 1.3 and absolute value of log2(fold-change(TG/WT)) ≥ 0.04, 781
337 phosphoproteins were differentially regulated by genotype. Of the 781 phosphoproteins, the
338 phosphorylation levels of 741 proteins were increased and only 40 were decreased in TGAC8 vs.
339 WT LV (Figure 1C).

340

341 **2. Functional analyses of the phosphoproteome.**

342 We performed the canonical pathway, upstream regulation, and downstream function analyses of
343 the remodeled LV phosphoproteome of TGAC8 using the Ingenuity Pathway Analysis (IPA)
344 software.

345 **2.1. Canonical pathway analysis of the remodeled LV phosphoproteome of TGAC8.**

346 To study the mechanisms at phosphorylation level, we first performed canonical pathway
347 analysis using IPA. Top canonical pathways within the phosphoproteome that were statistically
348 differentially enriched in TGAC8 vs. WT were displayed in the bar plot (Figure 1D and File 2:
349 Sheet 1). Of these pathways, cardiac hypertrophy signaling (enhanced) is most highly activated
350 (z-score as high as 4.867) (Figure 1D). The combination of Figure 1—figure supplement 1 and
351 File 2: Sheet 2 and our recently published work[5] showed that the phosphorylation status of
352 numerous molecules, e.g., Ca^{2+} ATPase, RyR2, Ncx, involved in excitation, calcium cycling,

353 contraction, relaxation and protein synthesis, was elevated in the TGAC8 vs. WT LV. However,
354 we have demonstrated that at three-month of age, the mouse age in the present study, the LV
355 mass is not elevated in TGAC8 vs. WT[5]. Of note, transcriptomic, proteomic and WB analyses
356 indicated that pathologic hypertrophic markers were not increased in TGAC8 vs. WT[5]. In this
357 regard, the activation of key stress response signaling pathways, e.g., protein kinase A (PKA)
358 signaling, PI3K signaling, and AMPK signaling, may protect against pathological changes, that
359 result in an increase in cardiac mass in TGAC8 despite its chronic increase in performance. For
360 example, activated PKA signaling can restrict the activity of AC8, acting as a feedback to fine-
361 tune the downstream signaling networks inside the body[14]. Additionally, nitric oxide (NO)
362 signaling may coordinate cardiac protection in the increase in cardiac mass (Figure 1D).
363 Increased phosphorylation status of HSP90 and Akt in TGAC8 synergistically increase eNOS
364 activity[15], and increased NO produced by eNOS may modulate the function of the ryanodine
365 receptor Ca^{2+} release channel (RyR2) on the cardiac sarcoplasmic reticulum[16]. The TMT-
366 labeling MS identified significant upregulated phosphorylation in the peptides of RyR2
367 (RISQTSQVSIDAAHGYSPR, E9Q401 [2805-2823]) (File 1: Sheet 1) , consistent with the PKA
368 induced phosphorylation of RyR2-S2809 mediating the increase in Ca^{2+} spark amplitude[17].

369 **2.2. Upstream regulators of the remodeled LV phosphoproteome of TGAC8.**

370 As known, the overexpression of AC8 activates the AC8-cAMP-PKA phosphorylation axis[4].
371 There were 2264 phosphosites whose names and locations are unambiguous within the 4990
372 upregulated phosphopeptides (p-value ≤ 0.05 and log2(fold-change(TG/WT)) ≥ 0) in TGAC8 vs.
373 WT. The majority of these phosphosites were serines (S) and threonines (T), and a few were
374 tyrosines (Y) (Figure 2A). By using WebLogo, we profiled the phosphorylation motif sequences
375 (Figure 2B). A typical PKA and AKT substate motif, R-R-X-pS/T, was the most abundant

376 substrate motif, consistent with increased PKA dependent phosphorylation (Figure 2B-2D)[18,19].
377 In addition to S and T, the center phosphosites also included phosphotyrosine (Y). The center
378 phosphosites were mainly flanked by the P-E-E sequence on the C terminus, endowing a strong
379 hydrophobic and acidic property to the C terminus of the substrate sequences (Figure 2B),
380 supported by the amphiphilicity index analysis in iceLogo (Figure 2D). Because phosphorylation
381 substrate motifs were not restricted to PKA's substrate motif, additional kinases must be also
382 involved in reprogramming the TGAC8 phosphoproteome. Therefore, we were inspired to
383 explore additional kinase-substrate pathways mediating the effect of the cardiac-overexpression
384 of AC8 here.

385 IPA predicted that 26 kinases were responsible for the above-mentioned phosphorylation motifs
386 (File 2: Sheet 3), among which, three had previously been identified to differ by genotype in the
387 LV transcriptome, 18 were shown to differ by genotype in the LV proteome, and 18 were
388 identified in the present phosphoproteome. Of note, most of the identified kinases were
389 upregulated in TGAC8 vs. WT at transcription, translation and PTM (phosphorylation) levels.
390 Within the phosphoproteome, eight kinases were predicted to be differentially activated by
391 genotype, and the phosphorylation level of four of these (PDPK1, PAK1, PTK2B and GSK3B)
392 was increased in TGAC8 vs. WT. These four kinases each phosphorylates various proteins to
393 regulate cellular functions. For example, a previous study observed that in human glioblastoma
394 cell lines, T98G and U87MG cells, the interference of human PDPK1 mRNA by siRNA
395 decreased the phosphorylation level of human BAD protein (S112, S136 and S155) and activated
396 cell death to suppress tumorigenesis[20]. Another study reported that in mouse myoblast cell line,
397 C2C12 cells, PDPK1 protein phosphorylated the mouse ULK1 protein[21]. Increased

398 phosphorylation states of BAD (upregulated at S112, S136 and S155) and ULK1 (upregulated at
399 S450, S521 and S637/638) in TGAC8 may be linked to activated PDPK1.

400 Different kinases can coordinate to reprogram the complex regulation network in the organism.
401 Consistent with the IPA canonical pathway analysis, the phosphorylation level of 27 proteins
402 (including the three kinases (PDPK1, PAK1 and PTK2B) auto-phosphorylating themselves)
403 were elevated by the three kinases to regulate cardiac stress signaling pathways, including PKA
404 signaling, ERK/MAPK signaling, cardiac hypertrophy signaling (enhanced), and renin-
405 angiotensin signaling (Figure 1E and Figure 1—figure supplement 2), to cope with the cardiac
406 stress in the TGAC8. For example, GSK3B is involved in multiple biological processes. PDPK1
407 phosphorylated GSK3B at S9[22,23] and PTK2B phosphorylated GSK3B at S9 and Y216[24,25] to
408 inhibit the kinase activity of GSK3B. In this phosphoproteome, GSK3B was phosphorylated at
409 multiple sites, including S9, Y216, S219 and S545, and thus GSK3B inhibition was linked to the
410 cardiac adaptation[26,27].

411 **2.3. Downstream functions of the remodeled LV phosphoproteome of TGAC8.**

412 To study the downstream functions of these phosphoproteins, we performed molecular and
413 cellular functions analysis in IPA. The enriched functions were mainly in three categories, i.e.,
414 cell viability, protein quality control, and metabolism (Figure 1F and File 2: Sheet5). The
415 functions of cellular assembly and organization, cellular function and maintenance, and cell
416 death and survival were ranked as the top three terms, indicating the important role of the
417 reprogrammed phosphoproteome in improving cell viability in response to the chronic stress of
418 the overexpression of AC8 in the mouse heart.

419

420 **3. Integrative analyses of transcriptome, proteome and phosphoproteome.**

421 We next integrated changes in PTM (phosphorylation) in TGAC8 vs. WT with genotypic
422 differences in protein translation and in transcription. The circos plot (Figure 3A) illustrates the
423 genotypic differences (TGAC8 vs. WT) in **molecules** identified across the transcriptome,
424 proteome, and phosphoproteome. In addition, the correlation scatter plots (Figure 3B)
425 demonstrated a moderate level of correlation of genotypic differences of molecular changes
426 within phosphoproteome and transcriptome, and a somewhat stronger correlation between
427 genotypic differences of molecular changes within phosphoproteome and proteome (Figure 3C).
428 Concordant and discordant enrichments of canonical pathways differed by genotype among the
429 three omics are shown in Figure 3D. A comparison of genotypic differences within the three
430 omics highlights the importance of protein phosphorylation, and the phosphorylation was
431 **coordinated with and supplemental to** transcription and translation.

432 Because kinases and phosphatases are the key regulators of phosphorylation, and
433 phosphorylation of transcription factors (TFs) are the primary determinant of their activities in
434 transcription, we compared genotypic differences in kinases, phosphatases and TFs within the
435 phosphoproteome and proteome with our previously published genotypic differences in the
436 TGAC8 vs. WT transcriptome[5] (Figure 3E). We identified 196 kinases, 71 phosphatases and 191
437 TFs in the present phosphoproteome (Figure 3F). The protein phosphorylation status of about
438 one half of these molecules differed significantly (p-value < 0.05) by genotype (Figure 3G), and
439 the protein phosphorylation status of majority of these molecules was increased (Figure 3H-3J).
440 The genotypic differences in the transcription (mRNA expression obtained from RNA-seq) and
441 translation (protein expression obtained from mass spectrometry) of these molecules, however,
442 differed from those in the phosphoproteome (Figure 3E). Because there were more molecules

443 that were unchanged or reduced in the TGAC8 vs. WT transcriptome or proteome than in the
444 phosphoproteome, it is clear that the changes in protein phosphorylation are of utmost
445 importance in the coordination of transcription, translation and PTM, that underlie the adaptive
446 response of the TGAC8 LV to the marked, chronic increase stress of its intrinsically activated
447 AC-cAMP-PKA-Ca^{2+} signaling. Thus, by utilizing multiple bioinformatic analysis methods, we
448 not only dissected the reprogrammed phosphoproteome and deduced its functions in the TGAC8
449 mouse LV, but also profiled the coordination of phosphoproteome, transcriptome and proteome.

450 **3.1. Implications of coordinated changes in protein phosphorylation and transcription in**
451 **TGAC8 vs. WT.**

452 The most likely type of coordination between protein phosphorylation and transcription is related
453 to phosphorylation states of TFs which is determined by kinases and phosphatases activities.
454 Analysis of the remodeled LV transcriptome of TGAC8 in Gene Ontology (GO) analysis using
455 DAVID online software discovered that enrichments of numerous phosphorylation and
456 dephosphorylation related biological processes and molecular functions significantly differed by
457 genotype (Figure 4A), and that the coordinated expression of numerous kinases and
458 phosphatases also differed by genotype (Figure 4B-4C and File 8). Because expression levels of
459 kinases and phosphatases do not denote their activation states, we utilized IPA to predict the
460 genotypic differences in activation states of upstream kinase and phosphatase (regulators of the
461 transcriptome). Intriguingly, 60 kinases were predicted to be upstream regulators of the
462 remodeled LV transcriptome of TGAC8, and the majority of these kinases were predicted to be
463 activated in TGAC8 vs. WT (Figure 4D and File 9). In contrast, much fewer phosphatases were
464 predicted between TGAC8 and WT, and most of these were predicted to be inhibited (Figure 4E
465 and File 9). Thus, the differential genotypic enrichment of phosphorylation status and predicted

466 activation of kinases and phosphatases identified in our post hoc analysis of our previously
467 reported TGAC8 vs. WT transcriptome[5] are linked to the differential genotypic reprogramming
468 of the phosphoproteome discovered in the present study.

469 We utilized IPA to predict the activation states of upstream transcription regulators on the basis
470 of the remodeled LV transcriptomes and proteomes, and then determined their expression levels
471 in transcriptome, proteome and phosphoproteome (Figure 4F). Because TFs are the main
472 regulators of transcription, and because phosphorylation of TFs usually regulates their
473 activities[28-30], we focused our subsequent analysis on functions of those TFs that were
474 differentially phosphorylated in TGAC8 vs. WT. To confirm the hypothesis that the TGAC8
475 might exert transcriptional control by TFs phosphorylation, we retrieved all TFs identified in our
476 previous transcriptome and proteome[5] and mapped them to the current phosphoproteome in order
477 to determine their genotypic differences in phosphorylation status. Of the 191 TFs also identified
478 in this phosphoproteome, 92 TFs differed significantly by genotype in phosphorylation status (p-
479 value < 0.05). In agreement with the general upregulated transcription in TGAC8 LV[5], nearly all
480 of the TFs that differed by genotype had increased phosphorylation level (Figure 4G and File 3).
481 The only exception was purine rich element binding protein G (Purg), known to be hyper-
482 phosphorylated in solid tumors[31].

483 We conducted Kyoto Encyclopedia of Genes and Genomes (KEGG) pathway analysis to further
484 probe the predicted facts of TFs that were generally hyper-phosphorylated in TGAC8 vs. WT.
485 Numerous immunity related pathways, cancer related pathways, and metabolism related
486 pathways were enriched (Figure 4H and File 4). We then utilized IPA for in-depth analysis.
487 Numerous metabolic canonical pathways (glucocorticoid receptor signaling and PPAR
488 signaling), a cancer related canonical pathway (regulation of epithelial-mesenchymal transition

489 pathway), and immunity related canonical pathways (role of JAK1, JAK2 and TYK2 in
490 interferon signaling, IL-9 signaling, JAK/Stat signaling, etc.) were enriched (Figure 4I and File
491 5: Sheet 1). Intriguingly, the sumoylation pathway was markedly inhibited. Because both
492 sumoylation and phosphorylation are important PTMs in transcriptional regulation[32,33], it is
493 possible that the upregulated protein phosphorylation and inhibited protein sumoylation pathway
494 in TFs coordinately activate transcription and improve immunity in the TGAC8 LV. In addition,
495 cell viability and metabolism in molecular and cellular functions were enriched in TGAC8 vs.
496 WT (Figure 4J and File 5: Sheet 2), consistent with enrichments of aforementioned KEGG
497 pathways and IPA canonical pathways (Figure 4H and 4I).

498 Taken together, we have discovered the existence of substantial crosstalk between protein
499 phosphorylation and transcription in the TGAC8 LV: phosphorylation of TFs reprograms
500 immunity and metabolism related pathways and functions in the TGAC8 LV, likely serving to
501 maintain cell survival in response to the chronic stress of marked AC8 overexpression.

502 **3.2. Coordinated changes in protein expression and phosphorylation of the remodeled**
503 **proteome and phosphoproteome of TGAC8.**

504 Having discovered the coordinated changes in the remodeled TGAC8 transcriptome and
505 phosphoproteome (Figure 4A-4E), we next sought to discover the extent to which changes in the
506 remodeled phosphoproteome of the TGAC8 LV were coordinated with changes in its remodeled
507 proteome. Numerous biological processes and molecular functions that were related to
508 phosphorylation and dephosphorylation were enriched in the remodeled TGAC8 LV proteome
509 (Figure 5A), as were numerous kinases and phosphatases (Figure 5B-5C and File 10). Twenty-
510 nine kinases that differed by genotype were predicted to be upstream regulators of the proteome,
511 and most of these were predicted to be activated in TGAC8 vs. WT. Fewer phosphatases than

512 kinases that differed by genotype were identified as upstream regulators of the remodeled
513 TGAC8 LV proteome (Figure 5D-5E and File 11).

514 One strategy adopted to probe deeper into the coordinated changes in the proteome and
515 phosphoproteome of the TGAC8 LV was to normalize the phosphoproteome to the total
516 proteome (in other words, to divide the phosphorylation expression by protein expression) (File
517 1: sheet4). Of the 3927 phosphoproteins identified in our mouse LV samples, 2164 were
518 identified in both the proteome and phosphoproteome, and these were focused for subsequent
519 analyses. After normalization, WT and TGAC8 samples manifested clear genotypic differences
520 in PCA analysis (Figure 5G), and phosphorylation status of numerous proteins normalized to the
521 protein expression level still differed by genotype without cutoff (Figure 5H) and with cutoff (-
522 log(p-value) > 1.3 and absolute(log2(TG/WT)) ≥ 0.4) (Figure 5I). Even after normalizing the
523 phosphorylation level to the protein expression level, the enrichments of canonical pathways in
524 TGAC8 were quite consistent with those of unnormalized phosphoproteome (Figure 5J and File
525 6). Cardiac hypertrophy signaling (enhanced) and cardiac hypertrophy signaling took the top two
526 places, emphasizing the important role of phosphorylation in the regulation of cardiac functions
527 in response to chronic stress when coordinated with changes in the total proteome.

528 Many important stress-response signaling pathways were enriched from phosphoproteome, e.g.,
529 PKA signaling, ERK/MAPK signaling, insulin receptor signaling, and PI3K/AKT signaling
530 (Figure 6A). Three of these pathways, PI3K/AKT, ERK/MAPK and ubiquitin labeling, were also
531 markedly enriched in our previous analysis on total proteome in TGAC8 LV[5]. By integrating and
532 comparing the enrichments from transcriptome, proteome and phosphoproteome, we were able
533 to identify the three signaling pathways in the TGAC8 LV, PI3K/AKT, ERK/MAPK and
534 ubiquitin labeling, that were regulated concordantly in transcription, translation, and PTM

535 (phosphorylation) (Figure 6B). WB validated activation of PI3K/AKT signaling pathway in
536 TGAC8, reproducing the results of our prior study using different antibodies (Figure 6C-6D and
537 Figure 6—figure supplement 1A (more significant)). We also demonstrated in that study that
538 ERK/MAPK signaling was also activated in TGAC8 vs. WT (Figure 6—figure supplement 1B-
539 C). Activation of PI3K/AKT and ERK/MAPK signaling is crucial for enhanced protein quality
540 control (the increase in protein synthesis and degradation) in the TGAC8 LV[5] (Figure 6—figure
541 supplement 1D- G). Although protein ubiquitination, an important process in protein
542 degradation, was enriched in TGAC8 LV within IPA analysis, its activity could not be predicted
543 on the basis of present knowledge base of IPA. Its WB analysis, however, indicated that
544 ubiquitination is indeed increased in TGAC8 vs. WT (Figure 6E).

545 We next sought to identify which molecules linked to PI3K/AKT signaling (one of the most
546 important pathways in this mouse model) differed in TGAC8 vs. WT. Among the significantly
547 changed upstream molecules, the majority were upregulated. AKT, a central molecule in the
548 pathway, was also increased in proteome and phosphoproteome (Figure 6F). By searching and
549 mapping the substrates of AKT, we unraveled that the phosphorylation levels of AKT peptide
550 substrates were mostly elevated in TGAC8 vs. WT (Figure 6G). Therefore, the downstream
551 effects and functions of AKT signaling were activated in TGAC8 LV: (1) upregulating GSK3 to
552 improve energy metabolism; (2) activating mTOR pathway to increase protein synthesis and cell
553 growth; (3) promoting NF-κB mediated transcription; (4) upregulating BAD and eNOS only at
554 phosphorylation level to enhance cell survival and cardiovascular functions. In summary, to
555 adapt the heart to stress for improved survival, the TGAC8 reprogram the cardiac LV
556 phosphoproteome to a large degree.

557

558 **4. Discordant regulation of the phosphoproteome and proteome in TGAC8 LV.**

559 Among the 443 proteins that differed by genotype in both protein phosphorylation and protein
560 expression levels, 33 were changed discordantly at the two levels (in opposite directions, i.e.,
561 upregulated in proteome but downregulated in phosphoproteome, or vice versa) (Figure 7A and
562 File 7: Sheet 1). We uploaded the 33 discordant proteins into STRING online software for
563 functional analyses. The GO_CC (Cellular Component) analysis resulted in many
564 **mitochondrial components**, indicating the involvement of phosphorylated proteins in
565 mitochondria (Figure 7B and File 7: Sheet 2). Reactome pathway analysis showed that in
566 addition to mitochondria, metabolic pathways were enriched significantly in TGAC8 (Figure 7C
567 and File 7: Sheet 3). Mitochondria are the hub of metabolism and multiple metabolic processes
568 are executed in mitochondria. Consistently, both metabolism and mitochondria related processes
569 were ranked the top processes in GO_BP (Biological Process) analysis (Figure 7D and File 7:
570 Sheet 4). Therefore, the discordant part between total proteome and phosphoproteome indicated
571 that the phosphorylation plays a critical role in the regulation of mitochondria and metabolism in
572 the TGAC8, distinct from its role in regulation at the translational level.

573

574 **5. Deduced schematic of coordination of phosphoproteome with transcriptome and**
575 **proteome in TGAC8 mouse LV.**

576 A deduced schematic integration of the remodeled phosphoproteome, proteome and
577 transcriptome of the TGAC8 LV is shown in Figure 8. The TGAC8 mouse initially induces a
578 PKA dependent phosphorylation via AC8-cAMP-PKA axis. Many cytoplasmic proteins
579 including TFs are thus phosphorylated and then transported into the nucleus where TFs

580 recognize and bind to the promoters to activate the transcription of more regulatory factors,
581 including kinases, phosphatases, and TFs. The activation states of these factors are changed upon
582 phosphorylated in cytosol, thereby activating additional kinases-controlled phosphorylation
583 cascades and reprogramming the cardiac phosphoproteome comprehensively.

584

585 **Discussion**

586 The major novel findings of the present study were differentially regulated phosphoproteins by
587 genotype and the enrichment of numerous stress-response pathways within the reprogrammed
588 TGAC8 LV, including PKA, PI3K and AMPK signaling pathways, their predicted upstream
589 regulators (e.g., PDPK1, PAK1 and PTK2B), and downstream functions (e.g., cell viability,
590 protein quality control, and metabolism). In addition to PKA, numerous other kinases and
591 phosphatases were hyper-phosphorylated in TGAC8 vs. WT. Hyper-phosphorylated
592 transcriptional factors in TGAC8 were associated with increased mRNA transcription, immune
593 responses and metabolic pathways. Integration of the phosphoproteome with its proteome and
594 with the previously published TGAC8 transcriptome enabled the elucidation of cardiac
595 performance and adaptive protection profiles that were coordinately regulated at PTM
596 (phosphorylation), translational and transcriptional levels. Many stress-response signaling
597 pathways, i.e., PI3K/AKT, ERK/MAPK and ubiquitin labeling, were consistently enriched and
598 activated in the TGAC8 LV at transcriptional, translational and PTM levels.

599 Most previous studies of PKA-dependent phosphorylation via the AC8-cAMP-PKA axis (typical
600 substrate motif of PKA dependent phosphorylation) focused on PKA phosphorylated targets as
601 downstream effects of activated AC8. For example, AC8 induced cAMP activates PKA to

602 increase the phosphorylation of many key proteins in cardiovascular system, e.g., ryanodine-
603 receptor-type 2 (RyR2), L-type Ca^{2+} channels (LTCC), phospholamban (PLN or PLB), etc[5]. Our
604 study identified 29 phosphosites on RyR2, 15 phosphosites on LTCC alpha 1 and beta 2, and 2
605 phosphosites (S16 and T17) on PLN, and, most interestingly, 7 phosphosites on SERCA2
606 (Sarcoplasmic/endoplasmic reticulum calcium ATPase 2), with the majority of these increased in
607 phosphorylation statuses in the TGAC8 LV (File 1: Sheet 1). It is worth noting that PLN is
608 phosphorylated on S16 by PKA whereas on T17 by Ca^{2+}-calmodulin-dependent protein kinase
609 (CaMKII)[34].

610 Following phosphorylation, many cytoplasmic proteins, including TFs, are transported into the
611 nucleus. TFs recognize and bind to the promoters to activate transcription, and many TFs were
612 hyper-phosphorylated in TGAC8 vs. WT (Figure 4 F and 4G). The phosphorylation of
613 STAT1[35,36], STAT3[36], HTT[37] and CREB1[38] is associated with the activation of their
614 transcriptional activities. Elevated TFs phosphorylation and possibly activated transcription were
615 consistent with the general increase in transcriptome in TGAC8[5]. The hyper-phosphorylated TFs
616 might contribute to the improved immunity, metabolism and cell viability in TGAC8 (Figure 4H
617 and 4I). For example, STAT family proteins are transcription activators, and their
618 phosphorylation is involved in inflammation and immune response[39,40]. The present study
619 identified increased phosphorylation levels in S727 on STAT1 and S726/S727 on STAT3 (File
620 1: Sheet 1), in line with our previous report which identified hyper-phosphorylation of
621 components within inflammation and immune response signaling pathways such as JAK/STAT
622 and JNK pathways[5].

623 Upon activation of RNA transcription, expression of numerous molecules, including TFs,
624 kinases, and phosphatases was increased in TGAC8 vs WT, thereby, leading to activation of

625 other kinase-controlled phosphorylation cascades in addition to PKA. For example, among the
626 others, IPA predicted activation of PDPK1, PAK1 and PTK2B directed signaling in TGAC8 vs
627 WT. In the context of the overexpression of AC8, these three kinases could be activated to
628 phosphorylate multiple proteins to activate the PKA pathway (positive feedback) and the
629 MAPK/ERK pathway (also known as Ras-Raf-MEK-ERK pathway) to maintain heart health
630 (Figure 1E and Figure 1—figure supplement 2). Previously, we showed WB results confirming
631 MAPK/ERK pathway activation due to increased protein expression of p21 Ras and the elevated
632 phosphorylation levels of c-Raf, MEK1/2 and ERK1/2 as well as their increased ratios of
633 phosphorylation to protein expression[5]. In the present study, S233 and S621/S641 on Isoform 2
634 of RAF proto-oncogene serine/threonine-protein kinase were hyper-phosphorylated in TGAC8
635 (File 1: Sheet 1). Importantly, the multifunctional molecule, GSK3B, was downstream of PDPK1
636 and PTK2B in the integrated regulation network. GSK3B is involved in metabolism and cardiac
637 hypertrophy[41,42]. Interestingly, AC8 is required for glucose homeostasis and hypothalamic
638 adaptation to high-fat diet[43]. The phosphorylation of GSK3B is also a critical mediator in
639 convergence of cardioprotection signaling[26,27]. We previously detected the increase in the protein
640 expression of GSK3B[5] and here identified the hyper-phosphorylated S9 on GSK3B (File 1: Sheet
641 1).

642 Taken together, the TGAC8 upregulates phosphorylation to reprogram the heart. Based on
643 results in this study, combined with our recently published work on TGAC8 LV[5], we generated a
644 comprehensive circuitry (Appendix-figure 1). Navigating this figure "by the numbers": marked,
645 chronic, cardiac specific overexpression of AC8 (1) chronically increases cAMP (2) and PKA-
646 Ca^{2+} signaling (3), resulting, not only in an incessantly increased cardiac performance, due to
647 elevated heart rate and LV contractility (4), but also activation of growth factor signaling

648 pathways (5), leading to increase in energy demand due to increased transcription and increased
649 amino acid, nucleotide, protein, lipid and lipoprotein synthesis, increased protein quality control,
650 including proteosome activity, autophagy, mitophagy, cytokine signaling and inflammation (6).
651 Chronic high level of AC8 activation elicits numerous stress responses (8) including increased
652 nutrient sensing with increased AMPK signaling (10A), increased ROS scavenging, protection
653 against cell death, and also induction of signaling to minimize the impact of AC-PKA signaling
654 (10B). Shifts in energy production and utilization to deal with the marked energy demands of the
655 TGAC8 heart (10, 12) include: enhancement of glucose metabolism is pronounced (11, 13),
656 whilst utilization of fatty acids to produce energy is reduced (11) but an increase in glucose
657 catabolism (10, 11) is accompanied by an increased anabolism (12), supported by increased
658 aerobic glycolysis (11,13); increased utilization of the pentose phosphate shunt (5, 13) supports
659 increased amino acid, nucleotide, protein and lipoprotein synthesis induced by growth factor
660 signaling (5), resulting in an increase in LV biomass (14). This adaptive profile balances energy
661 requirements necessary for an incessant marked increase in cardiac performance (4), for
662 increased RNA transcription, protein translation and quality control required for cardiac growth
663 (14), and for other biological processes within the LV myocardium (6). This pattern of consilient
664 adaptations (6-15) sustains an incessant increase in cardiac performance while conferring cardio-
665 protection to the TGAC8 heart.

666 **Summary and Future Perspectives**

667 The reprogrammed phosphoproteome activated stress response signaling pathways to defend
668 against cardiac stress in young mice, improve cell viability and suppress cell death. On one hand,
669 the reprogramed phosphoproteome enhances transcription to improve the immunity and
670 metabolism; on the other hand, it coordinates with the proteome to improve mitochondrial

671 functions and metabolism. Finally, although we revealed the coordination of regulation at
672 different levels, which provides a roadmap to guide the integration of transcription, translation
673 and PTM, our results set the stage for additional studies in this remarkable TGAC8 model: What
674 kinases are specifically involved in the PTM identified here? How are these phosphorylated
675 proteins specifically distributed in subcellular locations? Also, the specific details of how
676 PDPK1, PAK1 and PTK2B directed signaling is activated by overexpression of AC8 requires
677 further study. The bioinformatic analysis strategy here revealed a larger kinase-substrate network
678 important in the remodeling of the TGAC8 heart. We plan to validate these kinase-substrate
679 reactions in additional follow-up studies and provide the reliable mechanism in cardiovascular
680 research.

681 The present study focuses on a comprehensive in silico analysis of functionally coherent and
682 data-driven transcription, translation, and post-translation patterns that were well translated in the
683 contribution to AC8-overexpression cardiac outcomes, while further investigation is warranted to
684 see whether the hub pathway/function predictions via gene sets, phosphopeptides, and
685 phosphoproteins could be used as biomarkers or impact the diagnostic specificity for transgenic
686 AC8 cardiac health and pathology, and even be used as therapeutic targets to enhance heart
687 adaptivity, maintaining heart performance while avoiding cardiac dysfunction.

688

689 **Acknowledgements**

690 We thank all members in Laboratory of Cardiovascular Science, National Institute on Aging,
691 National Institutes of Health, for technical assistance and discussion. This work utilized the
692 computational resources of the NIH HPC Biowulf cluster (http://hpc.nih.gov).

Funding

Intramural Research Program, National Institute on Aging, National Institutes of Health.

Disclosures

None.

References

1 Lipskaia, L. *et al.* Enhanced cardiac function in transgenic mice expressing a Ca(2+)-stimulated adenylyl cyclase. *Circ. Res.* **86**, 795-801 (2000). https://doi.org:10.1161/01.res.86.7.795

2 Georget, M. *et al.* Augmentation of cardiac contractility with no change in L-type Ca2+ current in transgenic mice with a cardiac-directed expression of the human adenylyl cyclase type 8 (AC8). *Faseb j* **16**, 1636-1638 (2002). https://doi.org:10.1096/fj.02-0292fje

3 Esposito, G. *et al.* Increased myocardial contractility and enhanced exercise function in transgenic mice overexpressing either adenylyl cyclase 5 or 8. *Basic Res Cardiol* **103**, 22-30 (2008). https://doi.org:10.1007/s00395-007-0688-6

4 Moen, J. M. *et al.* Overexpression of a Neuronal Type Adenylyl Cyclase (Type 8) in Sinoatrial Node Markedly Impacts Heart Rate and Rhythm. *Front Neurosci* **13**, 615 (2019). https://doi.org:10.3389/fnins.2019.00615

5 Tarasov, K. V. *et al.* A remarkable adaptive paradigm of heart performance and protection emerges in response to the constitutive challenge of marked cardiac-specific overexpression of adenylyl cyclase type 8. *eLife* **11**, e80949 (2022). https://doi.org:10.7554/eLife.80949

6 Qu, J.-H. *et al.* Proteomic Landscape and Deduced Functions of the Cardiac 14-3-3 Protein Interactome. *Cells* **11**, 3496 (2022). https://doi.org:10.3390/cells11213496

7 Zhang, R. *et al.* Caloric Restriction Induces MicroRNAs to Improve Mitochondrial Proteostasis. *iScience* **17**, 155-166 (2019). https://doi.org:https://doi.org/10.1016/j.isci.2019.06.028

8 Pei, J. F. *et al.* Diurnal oscillations of endogenous H(2)O(2) sustained by p66(Shc) regulate circadian clocks. *Nature cell biology* **21**, 1553-1564 (2019). https://doi.org:10.1038/s41556-019-0420-4

9 Deng, C., Qu, J.-H., Kim, I. & Tang, X. Histone crotonylation in neurobiology: to be or not to be? *Chin. Med. J.* **135**, 1036-1038 (2022). https://doi.org:10.1097/cm9.0000000000001945

10 Consortium, T. U. UniProt: a worldwide hub of protein knowledge. *Nucleic Acids Res.* **47**, D506-D515 (2018). https://doi.org:10.1093/nar/gky1049

11 Crooks, G. E., Hon, G., Chandonia, J. M. & Brenner, S. E. WebLogo: a sequence logo generator. *Genome research* **14**, 1188-1190 (2004). https://doi.org:10.1101/gr.849004

12 Colaert, N., Helsens, K., Martens, L., Vandekerckhove, J. & Gevaert, K. Improved visualization of protein consensus sequences by iceLogo. *Nat Methods* **6**, 786-787 (2009). https://doi.org:10.1038/nmeth1109-786

13 Mitaku, S., Hirokawa, T. & Tsuji, T. Amphiphilicity index of polar amino acids as an aid in the characterization of amino acid preference at membrane-water interfaces. *Bioinformatics* **18**, 608-616 (2002). https://doi.org:10.1093/bioinformatics/18.4.608

14 Willoughby, D. *et al.* A key phosphorylation site in AC8 mediates regulation of Ca(2+)-dependent cAMP dynamics by an AC8-AKAP79-PKA signalling complex. *J Cell Sci* **125**, 5850-5859 (2012). https://doi.org:10.1242/jcs.111427

15 Takahashi, S. & Mendelsohn, M. E. Synergistic activation of endothelial nitric-oxide synthase (eNOS) by HSP90 and Akt: calcium-independent eNOS activation involves formation of an HSP90-Akt-CaM-bound eNOS complex. *The Journal of biological chemistry* **278**, 30821-30827 (2003). https://doi.org:10.1074/jbc.M304471200

16 Lim, G., Venetucci, L., Eisner, D. A. & Casadei, B. Does nitric oxide modulate cardiac ryanodine receptor function? Implications for excitation-contraction coupling. *Cardiovasc Res* **77**, 256-264 (2008). https://doi.org:10.1093/cvr/cvm012

17 Meissner, G. in *Structure and Function of Calcium Release Channels Current Topics in Membranes* 91-113 (2010).

18 Hunzicker-Dunn, M. E. *et al.* PKA and GAB2 play central roles in the FSH signaling pathway to PI3K and AKT in ovarian granulosa cells. *Proceedings of the National Academy of Sciences of the United States of America* **109**, E2979-2988 (2012). https://doi.org:10.1073/pnas.1205661109

19 Bellis, A. *et al.* Cross-talk between PKA and Akt protects endothelial cells from apoptosis in the late ischemic preconditioning. *Arterioscler Thromb Vasc Biol* **29**, 1207-1212 (2009). https://doi.org:10.1161/atvbaha.109.184135

20 Desai, S., Pillai, P., Win-Piazza, H. & Acevedo-Duncan, M. PKC-iota promotes glioblastoma cell survival by phosphorylating and inhibiting BAD through a phosphatidylinositol 3-kinase pathway. *Biochim Biophys Acta* **1813**, 1190-1197 (2011). https://doi.org:10.1016/j.bbamcr.2011.03.007

21 Li, Y. *et al.* microRNA-378 promotes autophagy and inhibits apoptosis in skeletal muscle. *Proceedings of the National Academy of Sciences of the United States of America* **115**, E10849-e10858 (2018). https://doi.org:10.1073/pnas.1803377115

22 Chen, X. *et al.* PDK1 regulates platelet activation and arterial thrombosis. *Blood* **121**, 3718-3726 (2013). https://doi.org:10.1182/blood-2012-10-461897

23 Ericson, K. *et al.* Genetic inactivation of AKT1, AKT2, and PDPK1 in human colorectal cancer cells clarifies their roles in tumor growth regulation. *Proceedings of the National Academy of Sciences of the United States of America* **107**, 2598-2603 (2010). https://doi.org:10.1073/pnas.0914018107

24 Hartigan, J. A., Xiong, W. C. & Johnson, G. V. Glycogen synthase kinase 3beta is tyrosine phosphorylated by PYK2. *Biochemical and biophysical research communications* **284**, 485-489 (2001). https://doi.org:10.1006/bbrc.2001.4986

25 Tsai, C. C. *et al.* Glycogen synthase kinase-3beta facilitates IFN-gamma-induced STAT1 activation by regulating Src homology-2 domain-containing phosphatase 2. *J Immunol* **183**, 856-864 (2009). https://doi.org:10.4049/jimmunol.0804033

26 Juhaszova, M. *et al.* Glycogen synthase kinase-3beta mediates convergence of protection signaling to inhibit the mitochondrial permeability transition pore. *The Journal of clinical investigation* **113**, 1535-1549 (2004). https://doi.org:10.1172/JCI19906

27 Juhaszova, M. *et al.* Role of glycogen synthase kinase-3beta in cardioprotection. *Circ. Res.* **104**, 1240-1252 (2009). https://doi.org:10.1161/CIRCRESAHA.109.197996

775 28 Bohmann, D. Transcription factor phosphorylation: a link between signal transduction and the
776 regulation of gene expression. *Cancer cells (Cold Spring Harbor, N.Y. : 1989)* **2**, 337-344 (1990).
777 29 Weigel, N. L. & Moore, N. L. Steroid receptor phosphorylation: a key modulator of multiple
778 receptor functions. *Molecular endocrinology (Baltimore, Md.)* **21**, 2311-2319 (2007).
779 https://doi.org:10.1210/me.2007-0101
780 30 Mayr, B. & Montminy, M. Transcriptional regulation by the phosphorylation-dependent factor
781 CREB. *Nature reviews. Molecular cell biology* **2**, 599-609 (2001).
782 https://doi.org:10.1038/35085068
783 31 Zanivan, S. *et al.* Solid tumor proteome and phosphoproteome analysis by high resolution mass
784 spectrometry. *J Proteome Res* **7**, 5314-5326 (2008). https://doi.org:10.1021/pr800599n
785 32 Tomanov, K. *et al.* Sumoylation and phosphorylation: hidden and overt links. *Journal of*
786 *Experimental Botany* **69**, 4583-4590 (2018). https://doi.org:10.1093/jxb/ery167
787 33 Khan, M. *et al.* Interplay between phosphorylation and SUMOylation events determines CESTA
788 protein fate in brassinosteroid signalling. *Nat Commun* **5**, 4687 (2014).
789 https://doi.org:10.1038/ncomms5687
790 34 Wegener, A. D., Simmerman, H. K., Lindemann, J. P. & Jones, L. R. Phospholamban
791 phosphorylation in intact ventricles. Phosphorylation of serine 16 and threonine 17 in response
792 to beta-adrenergic stimulation. *The Journal of biological chemistry* **264**, 11468-11474 (1989).
793 35 Pilz, A. *et al.* Phosphorylation of the Stat1 transactivating domain is required for the response to
794 type I interferons. *EMBO reports* **4**, 368-373 (2003). https://doi.org:10.1038/sj.embor.embor802
795 36 Wen, Z., Zhong, Z. & Darnell, J. E., Jr. Maximal activation of transcription by Stat1 and Stat3
796 requires both tyrosine and serine phosphorylation. *Cell* **82**, 241-250 (1995).
797 https://doi.org:10.1016/0092-8674(95)90311-9
798 37 Kumar, A., Vaish, M. & Ratan, R. R. Transcriptional dysregulation in Huntington's disease: a
799 failure of adaptive transcriptional homeostasis. *Drug Discov. Today* **19**, 956-962 (2014).
800 https://doi.org:10.1016/j.drudis.2014.03.016
801 38 Wang, H., Xu, J., Lazarovici, P., Quirion, R. & Zheng, W. cAMP Response Element-Binding Protein
802 (CREB): A Possible Signaling Molecule Link in the Pathophysiology of Schizophrenia. *Frontiers in*
803 *molecular neuroscience* **11**, 255-255 (2018). https://doi.org:10.3389/fnmol.2018.00255
804 39 Seif, F. *et al.* The role of JAK-STAT signaling pathway and its regulators in the fate of T helper
805 cells. *Cell Communication and Signaling* **15**, 23 (2017). https://doi.org:10.1186/s12964-017-
806 0177-y
807 40 Decker, T. & Kovarik, P. Serine phosphorylation of STATs. *Oncogene* **19**, 2628-2637 (2000).
808 https://doi.org:10.1038/sj.onc.1203481
809 41 Beurel, E., Grieco, S. F. & Jope, R. S. Glycogen synthase kinase-3 (GSK3): regulation, actions, and
810 diseases. *Pharmacol Ther* **148**, 114-131 (2015).
811 https://doi.org:10.1016/j.pharmthera.2014.11.016
812 42 Lal, H., Ahmad, F., Woodgett, J. & Force, T. The GSK-3 family as therapeutic target for myocardial
813 diseases. *Circ Res* **116**, 138-149 (2015). https://doi.org:10.1161/circresaha.116.303613
814 43 Raoux, M. *et al.* Multilevel control of glucose homeostasis by adenylyl cyclase 8. *Diabetologia*
815 **58**, 749-757 (2015). https://doi.org:10.1007/s00125-014-3445-z

816

817

818

819 **Figure Legends**

820 **Figure 1. TGAC8 reprograms the LV phosphorylation state. A**. PCA plot of
821 phosphoproteome in TGAC8 vs. WT LVs. **B**. Heatmap of scaled expressions of phosphorylated
822 proteins. **C**. Volcano plot of phosphoproteome. Red dots represent upregulated phosphoproteins
823 with -log10(p-value) > 1.3 and log2(fold change) ≥ 0.4; blue dots represent downregulated
824 phosphoproteins with -log10(p-value) > 1.3 and log2(fold change) ≤ -0.4; grey dots represent
825 nonsignificantly regulated phosphoproteins with -log10(p-value) ≤ 1.3 or absolute(log2(fold
826 change)) < 0.4. **D**. Top 21 canonical pathways enriched from phosphoproteome. Orange and blue
827 bars represent activated and inhibited pathways respectively. The darker the color is, the greater
828 the absolute(z-score) is, and the more significantly enriched the pathway is. **E**. Regulatory
829 pathway from upstream kinases. Three dots in the center represent the predicted upstream
830 kinases. Surrounding dots represent identified phosphoproteins differentially regulated in
831 phosphoproteome. Terms on the bottom represent canonical pathways in which the
832 phosphoproteins are involved. Meanings of colors refer to the box of prediction legend besides
833 the graph. **F**. Enriched molecular and cellular functions from the phosphoproteome. They are
834 related to three categories, including cell viability, protein quality control, and metabolism.

835

836 **Figure 1—figure supplement 1. The enriched pathway, Cardiac Hypertrophy Signaling**
837 **(Enhanced), from the phosphoproteome.** Cardiac Hypertrophy Signaling (Enhanced) is
838 visualized using IPA. Dots with purple outline are identified phosphoproteins or protein
839 complexes. Red and green fill colors indicate upregulation and downregulation respectively.

840

841 **Figure 1—figure supplement 2. The regulatory pathway under the control of a predicted**
842 **upstream kinase, PDPK1.** PDPK1 in the center is one representative of predicted upstream
843 kinases. Surrounding dots represent identified phosphoproteins differentially regulated in
844 phosphoproteome. Meanings of colors refer to the box of prediction legend besides the graph.
845 Blue glows represent that the increased phosphorylation levels inhibit the activity of
846 corresponding proteins.

847

848 **Figure 2. Characteristics of upregulated phosphopeptides. A**. Composition of phosphosites
849 that reside on the upregulated phosphopeptides. **B**. Sequence logo diagrams of upregulated
850 phosphopeptides centered on the phosphosites and flanked by 6 amino acids on the N and C
851 termini respectively using WebLogo online software. Colors of amino acids represent different
852 chemical properties. **C**. Western blots of phosphorylation of PKA substrates and their statistics
853 results: RRXS*/T*. Unpaired Student's t test with Welch's correction was used. **D**. Test the
854 amphiphilicity feature of the upregulated phosphopeptides using iceLogo online software and
855 referring to a published work by Mitaku and colleagues in 2002[13].

856

857 **Figure 3. Integrative analysis of transcriptome, proteome and phosphoproteome. A**. Circos
858 plot of gene expression at different levels from transcription, to protein, and to phosphorylation.
859 Bars in each layer of circle represent changes of significantly regulated molecules (q-value or p-
860 value < 0.05) in transcriptome, total proteome, and unnormalized phosphoproteome. Bar height,
861 color and direction represent log2(fold change). Red and upward indicate upregulation, and blue
862 and downward indicate downregulation. **B-C**. Scatter plots of correlation between

863 phosphoproteome and transcriptome (**B**) or total proteome (**C**). **D**. Comparison of canonical
864 pathway enrichments from the transcriptome, total proteome, and phosphoproteome. Enrichment
865 z-scores were calculated in IPA, and were scaled to generate heatmap in R language. **E**.
866 Integrative graph of expression of all phosphoproteins and selected types of molecules. Bar plot
867 on the bottom displays expression of all significantly changed (p-value < 0.05) phosphoproteins
868 in unnormalized phosphoproteome. Y-axis denotes log2(fold change), and x-axis denotes each
869 molecule ranked by log2(fold change). Bars were colored by -log10(p-value). Stick plots on the
870 top display kinases, phosphatases and transcription factors (TFs) selected from the bottom bar
871 plot and their changes in transcriptome (RNA), total proteome (pro), and normalized
872 phosphoproteome (norm). From top to bottom: each large block denotes the changes of certain
873 types of molecules (from kinases to phosphatases, to TFs). In each block, the three rows from top
874 to bottom indicate the changes in transcriptome, total proteome, and normalized
875 phosphoproteome. Each stick represents a molecule and color represents the change: red: (p-
876 value or q-value < 0.05) and log2FC > 0; blue: (p-value or q-value < 0.05) and log2FC < 0;
877 black: (p-value or q-value ≥ 0.05) or log2FC = 0; grey: unidentified in one of the omics. Their
878 locations are matched to those in the bottom bar plot. **F-J**. Pie plots of composition of
879 phosphoproteins in the unnormalized phosphoproteome. Regardless of p-value, numbers of four
880 types of proteins, including kinases, phosphatases, TFs and others, are displayed in **F**. After
881 filtration with cutoff p-value < 0.05, numbers of those types of proteins are displayed in **G**.
882 Extracted from G, numbers of upregulated and downregulated kinases (**H**), phosphatases (**I**) and
883 TFs (**J**) are displayed.

884

885 **Figure 4. Coordination of phosphoproteome and transcriptome. A**. GO term enrichments of
886 biological processes and molecular functions about phosphorylation and dephosphorylation from
887 transcriptome. **B-C**. Changes of kinases (**B**) and phosphatases (**C**) whose q-values are less than
888 0.05 in transcriptome. **D-E**. States of upstream kinases (**D**) and phosphatases (**E**) predicted based
889 on transcriptome. Z-scores were calculated in IPA. Positive and negative z-scores indicate
890 activated and inhibited states respectively. The larger absolute values of z-score indicate more
891 activated or inhibited states. **F**. Heatmap of predicted upstream transcription regulators (left) and
892 their changes in different omics datasets (right). Left: Fill color represent activation z-scores in
893 transcriptome and total proteome. Red and blue indicate activated and inhibited states
894 respectively. Molecules are ranked by z-scores in transcriptome. Right: Fill color represent
895 changes in transcriptome, total proteome, unnormalized phosphoproteome, and normalized
896 phosphoproteome: orange: (p-value or q-value < 0.05) and log2FC > 0; yellow: (p-value or q-
897 value ≥ 0.05) and log2FC > 0; green: (p-value or q-value < 0.05) and log2FC < 0; light blue: (p-
898 value or q-value ≥ 0.05) and log2FC < 0; grey: unidentified in one of the omics. **G**. Changes of
899 differentially regulated TFs with p-value < 0.05 in the unnormalized phosphoproteome. **H**.
900 KEGG pathway enrichments of the differentially regulated TFs. They are in four primary
901 categories: cancer, immunity, metabolism and others. **I**. Top 20 canonical pathways enriched
902 from the phosphoproteome using IPA. The darker the color is, the greater the absolute(z-score)
903 is, and the more significantly enriched the pathway is. **J**. Enriched molecular and cellular
904 functions from the phosphoproteome using IPA. They are in two primary categories: cell
905 viability and metabolism.

906

907 **Figure 5. Analysis of normalized phosphoproteome. A**. GO term enrichments of biological
908 processes and molecular functions about phosphorylation and dephosphorylation from the
909 present proteome. **B-C**. Changes of kinases (**B**) and phosphatases (**C**) whose q-values are less
910 than 0.05 in previous proteome. **D-E**. States of upstream kinases (**D**) and phosphatases (**E**)
911 predicted based on the present proteome. Z-scores were calculated in IPA. Positive and negative
912 z-scores indicate activated and inhibited states respectively. The larger absolute values of z-score
913 indicate more activated or inhibited states. **F**. Venn plot of new total proteome and unnormalized
914 phosphoproteome that were conducted concurrently in the same platform. **G**. PCA plot of
915 phosphoproteome normalized to total proteome. **H**. Heatmap of expressions of phosphoproteins
916 normalized to total proteins. **I**. Volcano plot of normalized phosphoproteome. Red dots represent
917 upregulated phosphoproteins with -log10(p-value) > 1.3 and log2(fold change) ≥ 0.4; blue dots
918 represent downregulated phosphoproteins with -log10(p-value) > 1.3 and log2(fold change) ≤ -
919 0.4; grey dots represent nonsignificantly regulated phosphoproteins with -log10(p-value) ≤ 1.3 or
920 absolute(log2(fold change)) < 0.4. **J**. Comparison of canonical pathway enrichments between
921 unnormalized and normalized phosphoproteome. Orange fill colors indicate that all comparable
922 pathways on the top are activated in both omics datasets. The darker the color is, the greater the
923 absolute(z-score) is, and the more significantly enriched the pathway is.

924

925 **Figure 6. Coordinated regulation of transcriptome, proteome and phosphoproteome on**
926 **PI3K/AKT and ERK/MAPK signaling pathways and protein synthesis and degradation. A**.
927 Canonical pathway enrichment of phosphoproteome only with cutoff p-value < 0.05. The darker
928 the color is, the greater the absolute(z-score) is, and the more significantly enriched the pathway
929 is. **B**. Comparison of PI3K/AKT signaling and protein ubiquitination pathways enriched from

930 transcriptome (red outline), proteome (blue outline) and phosphoproteome (green outline). **C-D**.
931 Western blots of two phosphorylation sites on pan-AKT protein for verification of
932 phosphorylation and activation of PI3K/AKT signaling pathway in TGAC8 vs. WT. **E**. Western
933 blot of ubiquitination in TGAC8 vs. WT. **F**. Pathway graph of PI3K/AKT signaling marked with
934 changes in transcriptome (left box), proteome (middle box) and phosphoproteome (right box).
935 Fill colors indicate changes: red and green indicate upregulation and downregulation
936 respectively; grey indicates nonsignificant regulation. **G**. Phosphopeptide number of substrates
937 of PI3K. Y-axis represents protein substates of PI3K; x-axis represents number of
938 phosphopeptides. Red and blue bars indicate upregulated (p-value < 0.05 and log2(fold
939 change) > 0) and downregulated (p-value < 0.05 and log2(fold change) < 0) phosphopeptides
940 respectively. Two-tailed unpaired Student's t test with Welch's correction was conducted and p-
941 values were shown in plots.

942

943 **Figure 6—figure supplement 1. Cross verification of activated PI3K/AKT and ERK/MAPK**
944 **signaling pathways and enhanced protein synthesis and degradation from our previous**
945 **study. A.** Western blots of one phosphorylation site on isoform 2 of AKT protein for verification
946 of phosphorylation and activation of PI3K/AKT signaling pathway in TGAC8 vs. WT. **B-C.**
947 Western blot verification of phosphorylation and activation of ERK/MAPK signaling pathway in
948 TGAC8 vs. WT. **D.** Confirmation of enhanced protein synthesis in TGAC8 vs. WT. **E.** The
949 enhanced proteasome activity in TGAC8 vs. WT. **F-G.** The soluble misfolded proteins were
950 increased in TGAC8 LV (**F**) whereas the insoluble protein aggregates did not accumulate within
951 the TGAC8 vs. WT (**G**). Two-tailed unpaired Student's t test with Welch's correction was

952 performed. P-values: * < 0.05, ** < 0.01, *** < 0.001, **** < 0.0001. These data were adapted
953 from our recently published study in TGAC8 and WT mice[5].

954

955 **Figure 7. Analyses of proteins changed discordantly in proteome and phosphoproteome. A**.
956 Venn diagram of significantly regulated proteins in total proteome and significantly regulated
957 phosphoproteins in unnormalized phosphoproteome that were conducted concurrently in the
958 same platform. **B-D**. Functional analyses of proteins whose expressions are changed discordantly
959 at total protein and phosphorylation levels. Mitochondria and others are enriched in cellular
960 component analysis (**B**). Functions related to metabolism, mitochondria and others are enriched
961 in Reactome pathway (**C**) and biological process analyses (**D**).

962

963 **Figure 8. Deduced schematic of coordination of phosphoproteome with transcriptome and**
964 **proteome in TGAC8 mouse LV.** Based on our results, we deduced a mechanism of
965 reprogramed phosphoproteome in TGAC8 mouse LV: First, TGAC8 mouse induces a PKA
966 dependent phosphorylation via AC8-cAMP-PKA axis. Many cytoplasmic proteins including TFs
967 are thus phosphorylated and then transported into the nuclear where TFs recognize and bind to
968 the promotors to activate the transcription of more regulatory factors, including kinases,
969 phosphatases, and TFs. The activation states of these factors are changed upon phosphorylated in
970 cytosol, thereby activating additional kinases-controlled phosphorylation cascades and
971 reprogramming the cardiac phosphoproteome comprehensively. Left column: AC8-cAMP-PKA
972 signaling; middle column: phosphorylation (phosphoproteome); lower right: transcription
973 (transcriptome); upper right: translation (proteome).

974

975 **Appendix-figure 1. Reprogrammed concentric performance and protection circuitry in**
976 **response to the constitutive challenge of marked cardiac-specific overexpression of adenylyl**
977 **cyclase type 8.** Based on the present phosphoproteome, we optimized our previously deduced
978 mechanism graph and labeled findings from the phosphoproteome using red stars. TGAC8
979 mouse induces a chronic cardiac exercise on heart, manifested as increased heart rate and
980 contractility accompanied with increased energy demand and cardiac biomass. Multiple
981 signaling pathways, related to nutrient sensing, energy production, cardiac cellular stress, cardiac
982 stress response, growth factor signaling, and cell proliferation, are potential downstream
983 mediating the effect of the activated AC8-cAMP-PKA-Ca^{2+} signaling in mouse LV. The altered
984 cardiac functions were also observed associated with protein phosphorylation in our previous
985 study and labeled in blue star here.

986

987 **Figures**

988 **Figure 1. TGAC8 reprograms the LV phosphorylation state.**

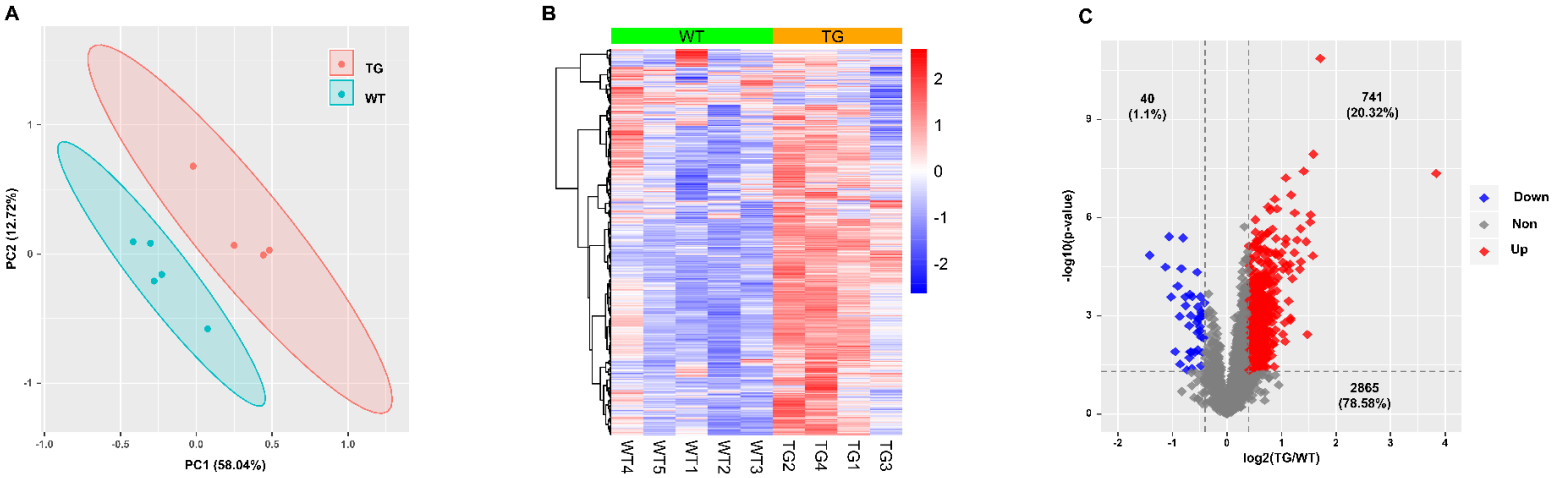
A
TG
WT
PC2 (12.72%)
PC1 (58.04%)
B
WT
TG
WT4
WT5
WT1
WT2
WT3
TG2
TG4
TG1
TG3
C
40
(1.1%)
741
(20.32%)
2865
(78.58%)
-log10(p-value)
log2(TG/WT)
Down
Non
Up

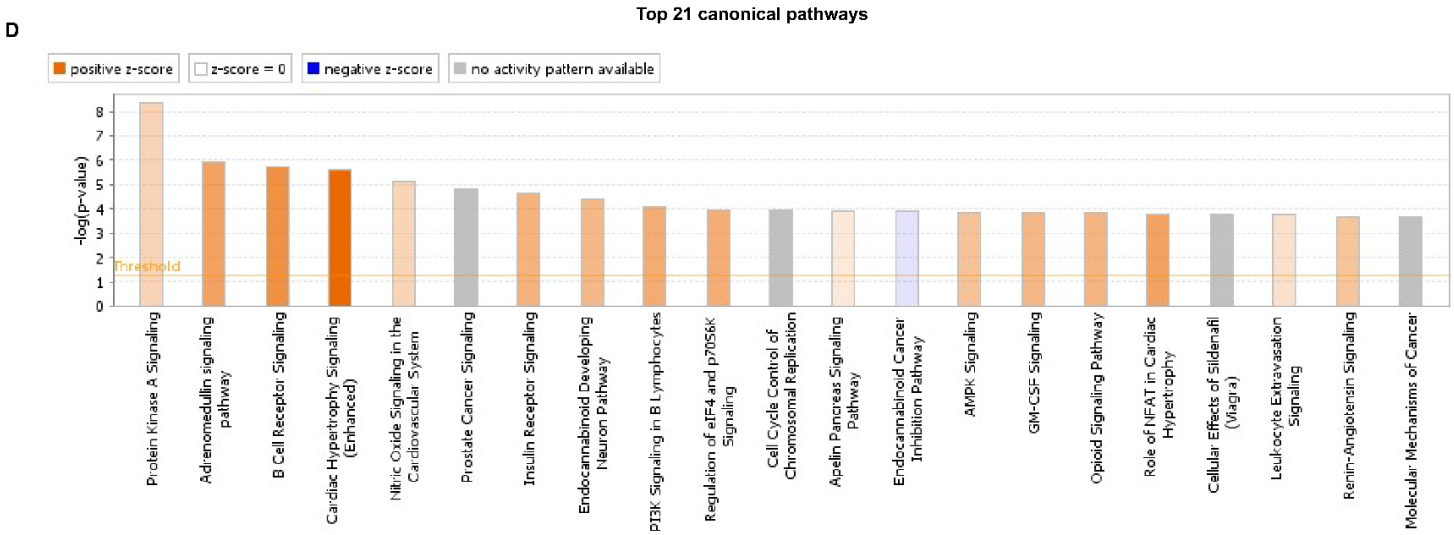
D
Top 21 canonical pathways
positive z-score
z-score = 0
negative z-score
no activity pattern available
-log(p-value)
Threshold
Protein Kinase A Signaling
Adrenomedullin signaling pathway
B Cell Receptor Signaling
Cardiac Hypertrophy Signaling (Enhanced)
Nitric Oxide Signaling in the Cardiovascular System
Prostate Cancer Signaling
Insulin Receptor Signaling
Endocannabinoid Developing Neuron Pathway
PI3K Signaling in B Lymphocytes
Regulation of eIF4 and p70S6K Signaling
Cell Cycle Control of Chromosomal Replication
Apelin Pancreas Signaling Pathway
Endocannabinoid Cancer Inhibition Pathway
AMPK Signaling
GM-CSF Signaling
Opioid Signaling Pathway
Role of NFAT in Cardiac Hypertrophy
Cellular Effects of Sildenafil (Magra)
Leukocyte Extravasation Signaling
Renin-Angiotensin Signaling
Molecular Mechanisms of Cancer

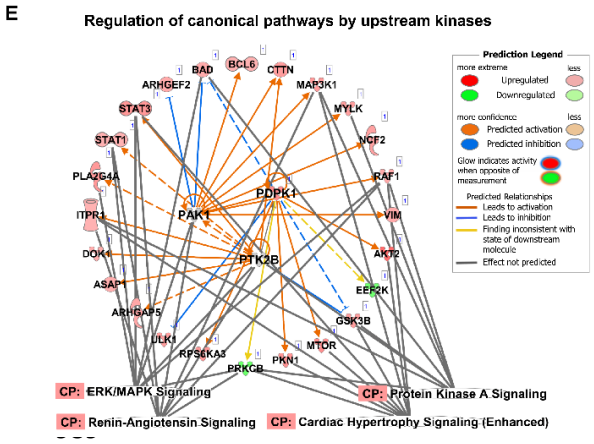
E
Regulation of canonical pathways by upstream kinases
Prediction Legend
Upregulated
Downregulated
Predicted activation
Predicted inhibition
Leads to activation
Leads to inhibition
Effect not predicted
BAD
BCL6
CTTN
ARHGEF2
MAP3K1
STAT3
MYLK
STAT1
NCF2
PLA2G4A
RAF1
PDPK1
ITPR1
PAK1
VIM
DOK4
PTK2B
AKT2
ASAP1
EEF2K
ARHGAP5
GSK3B
ULK1
MTOR
RPS6KA3
PKN1
PRKCB
CP: ERK/MAPK Signaling
CP: Protein Kinase A Signaling
CP: Renin-Angiotensin Signaling
CP: Cardiac Hypertrophy Signaling (Enhanced)

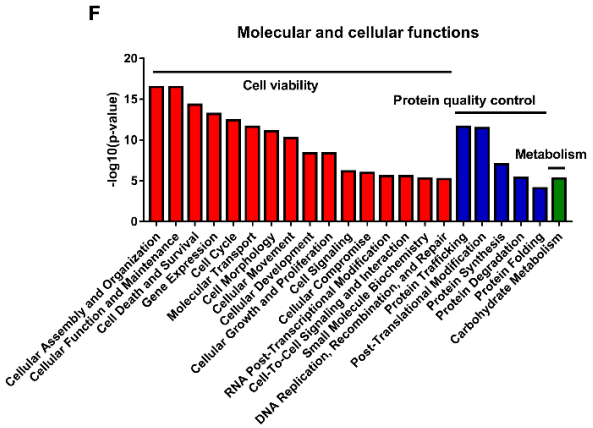
F
Molecular and cellular functions
-log10(p-value)
Cell viability
Protein quality control
Metabolism
Cellular Assembly and Organization
Cellular Function and Maintenance
Cell Death and Survival
Gene Expression
Cell Cycle
Molecular Transport
Cell Morphology
Cellular Movement
Cellular Development
Cellular Growth and Proliferation
Cell Signaling
Cellular Compromise
RNA Post-Transcriptional Modification
Small Molecule Biochemistry
Cell-To-Cell Signaling and Interaction
DNA Replication, Recombination, and Repair
Post-Translational Modification
Protein Trafficking
Protein Synthesis
Protein Degradation
Protein Folding
Carbohydrate Metabolism

990 **Figure 1—figure supplement 1. The enriched pathway, Cardiac Hypertrophy Signaling**

991 **(Enhanced), from the phosphoproteome.**

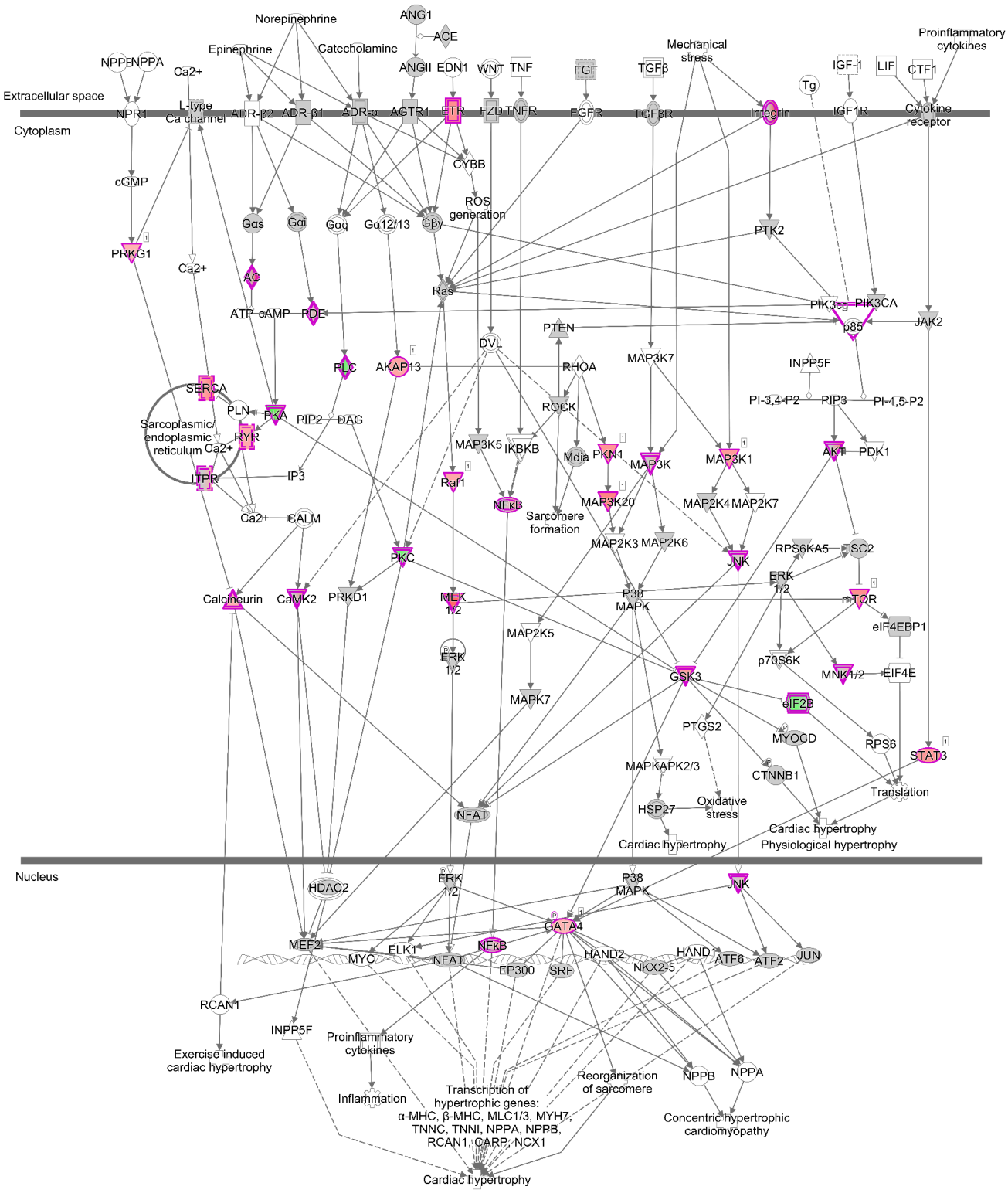

99

993 **Figure 1—figure supplement 2. The regulatory pathway under the control of a predicted**

994 **upstream kinase, PDPK1.**

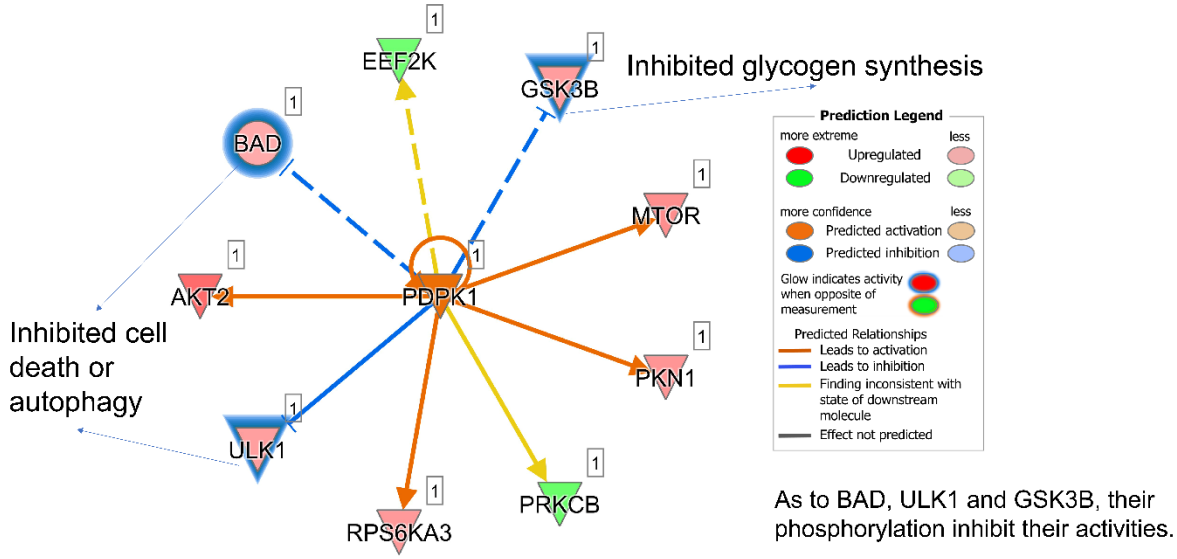

Symbol	Entrez Gene Name	UniProt	Log Ratio	p-value	Location	Family
AKT2	AKT serine/threonine kinase 2	Q60823	0.840825	0.007813	Cytoplasm	kinase
BAD	BCL2 associated agonist of cell death	Q61337	0.476462	7.81E-06	Cytoplasm	other
EEF2K	eukaryotic elongation factor 2 kinase	O08796	-0.42591	0.004744	Cytoplasm	kinase
GSK3B	glycogen synthase kinase 3 beta	Q9WV60	0.556065	0.002741	Nucleus	kinase
MTOR	mechanistic target of rapamycin kinase	Q9JLN9	0.640641	0.000144	Nucleus	kinase
PDPK1	3-phosphoinositide dependent protein kinase 1	Q9Z2A0	0.651174	0.02451	Cytoplasm	kinase
PKN1	protein kinase N1	P70268-2	0.600171	0.007485	Cytoplasm	kinase
PRKCB	protein kinase C beta	P68404-2	-0.44609	0.001011	Cytoplasm	kinase
RPS6KA3	ribosomal protein S6 kinase A3	P18654	0.580733	0.005794	Cytoplasm	kinase
ULK1	unc-51 like autophagy activating kinase 1	O70405	0.549454	0.015177	Cytoplasm	kinase

995

996

997

998

999

1000

1001

1002 **Figure 2. Characteristics of upregulated phosphopeptides.**

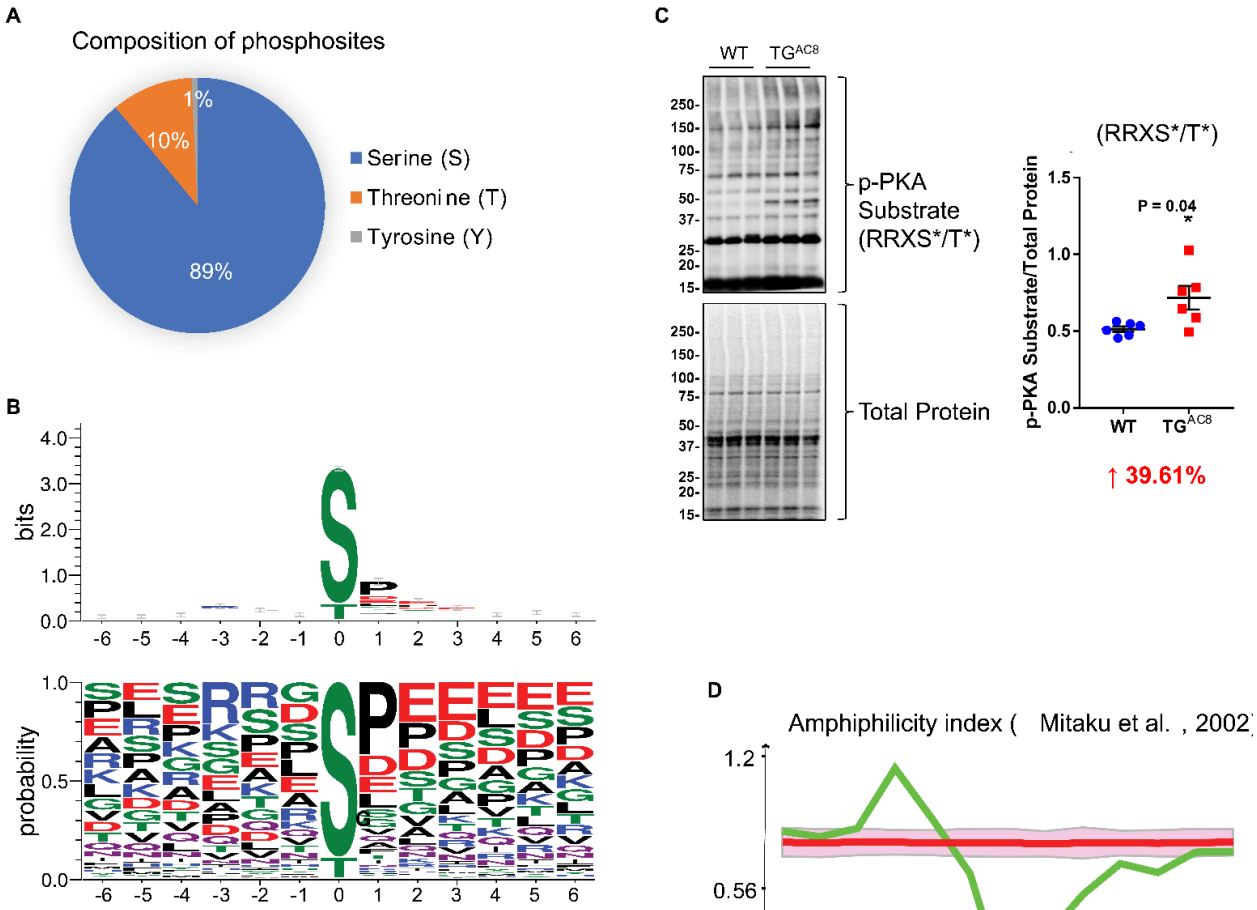

Polar	G,S,T,Y,C	green
Neutral	Q,N	purple
Basic	K,R,H	black
Acidic	D,E	red
Hydrophobic	A,V,L,I,P,W,F,M	black

1003

1004

1005

1006

1007

1008

1009 **Figure 3. Integrative analysis of transcriptome, proteome and phosphoproteome.**

1010

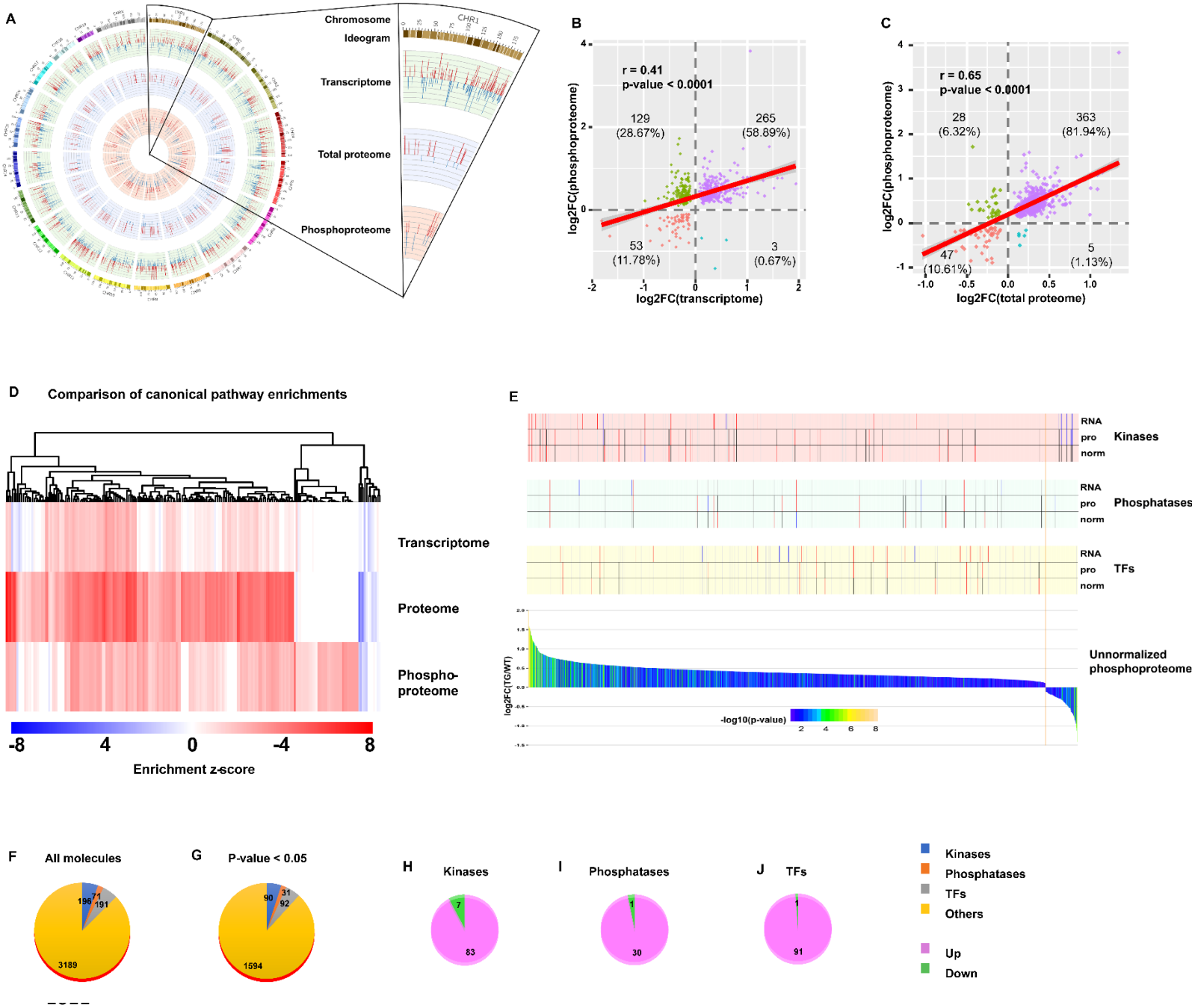

1012

1013

1014 **Figure 4. Coordination of phosphoproteome and transcriptome.**

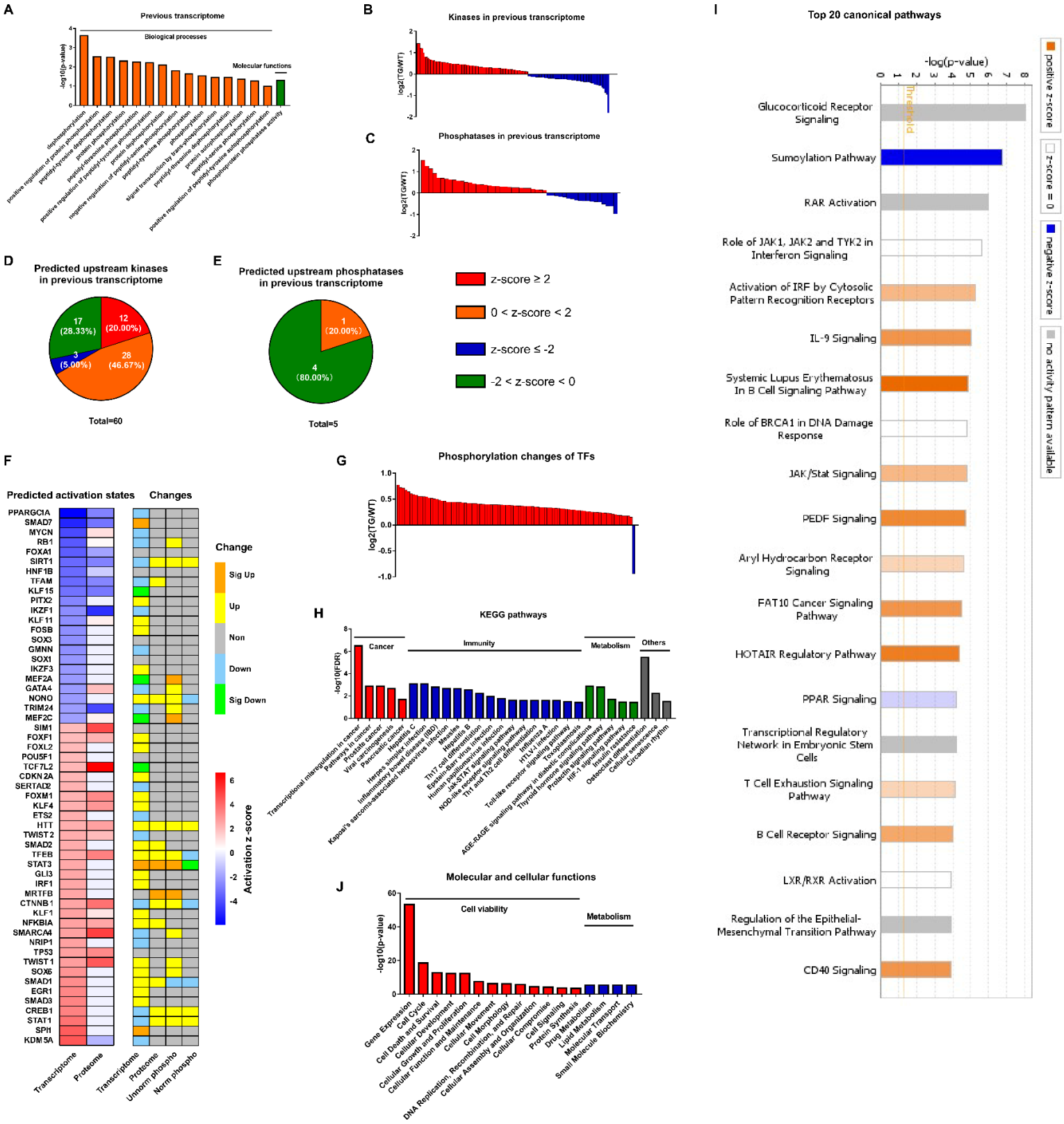

1016 **Figure 5. Analysis of normalized phosphoproteome.**

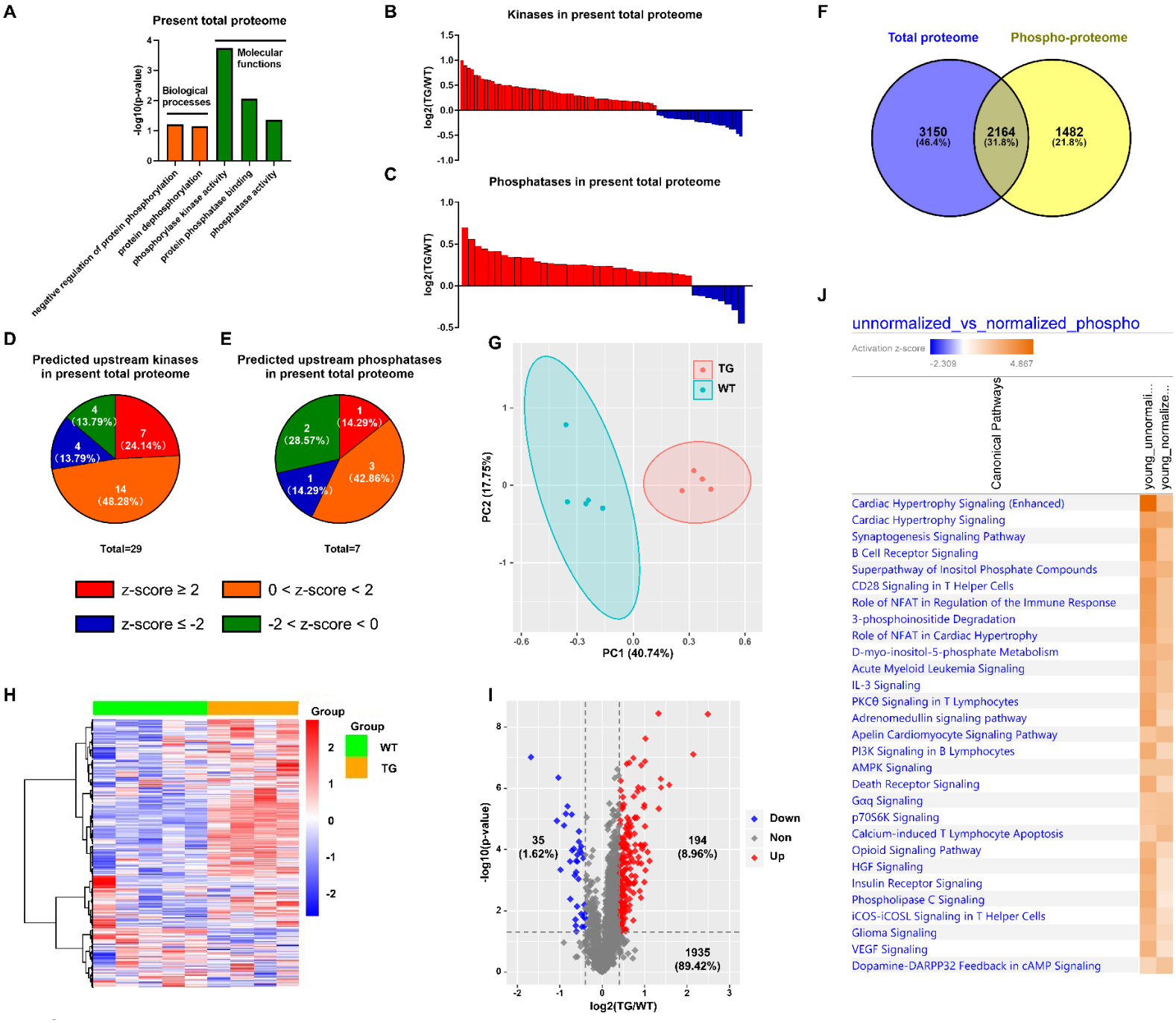

1018

1019

Figure 6. Coordinated regulation of transcriptome, proteome and phosphoproteome on PI3K/AKT and ERK/MAPK signaling pathways and protein synthesis and degradation.

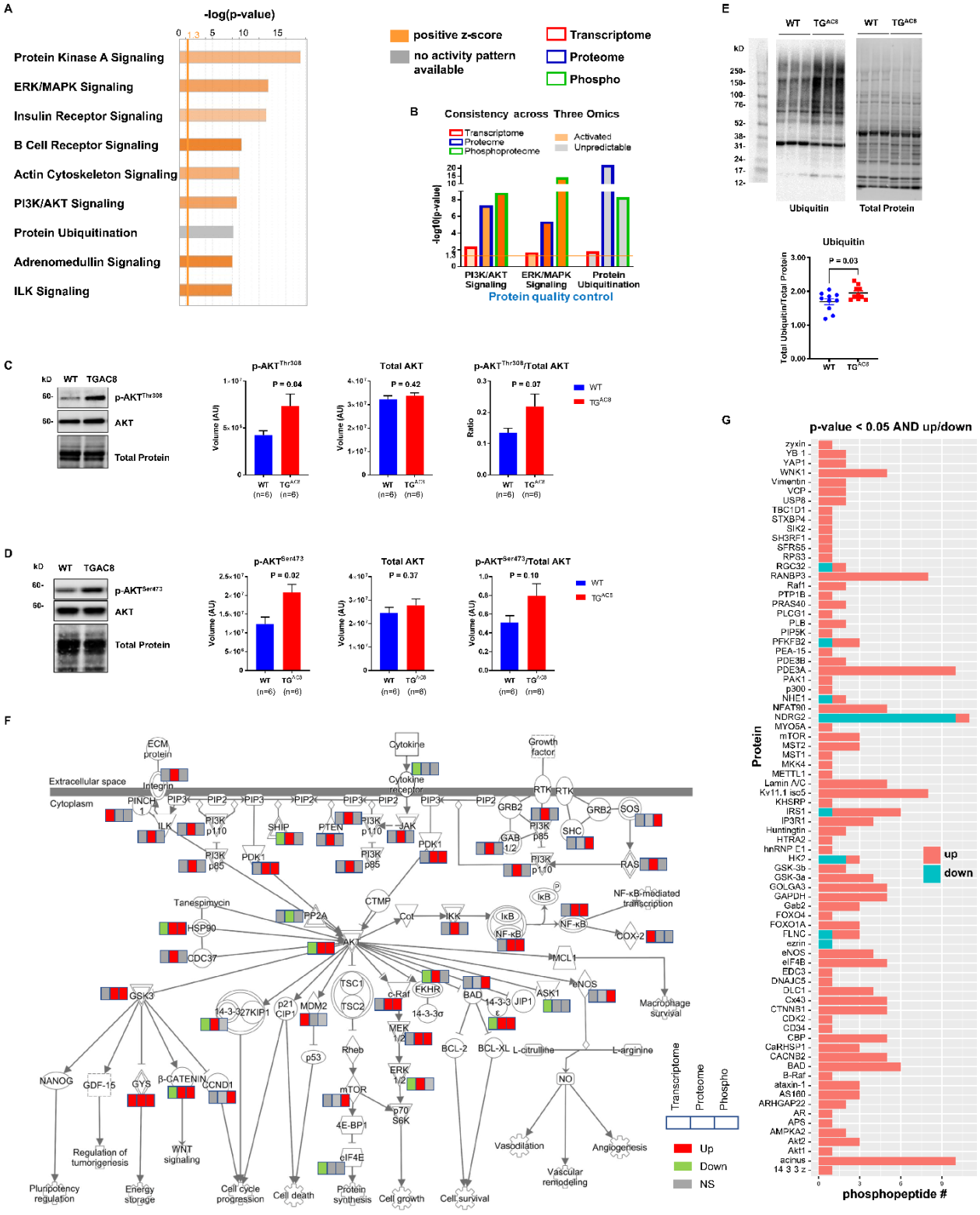

1023 **Figure 6—figure supplement 1. Cross verification of activated PI3K/AKT and ERK/MAPK**

1024 **signaling pathways and enhanced protein synthesis and degradation from our previous**

1025 **study.**

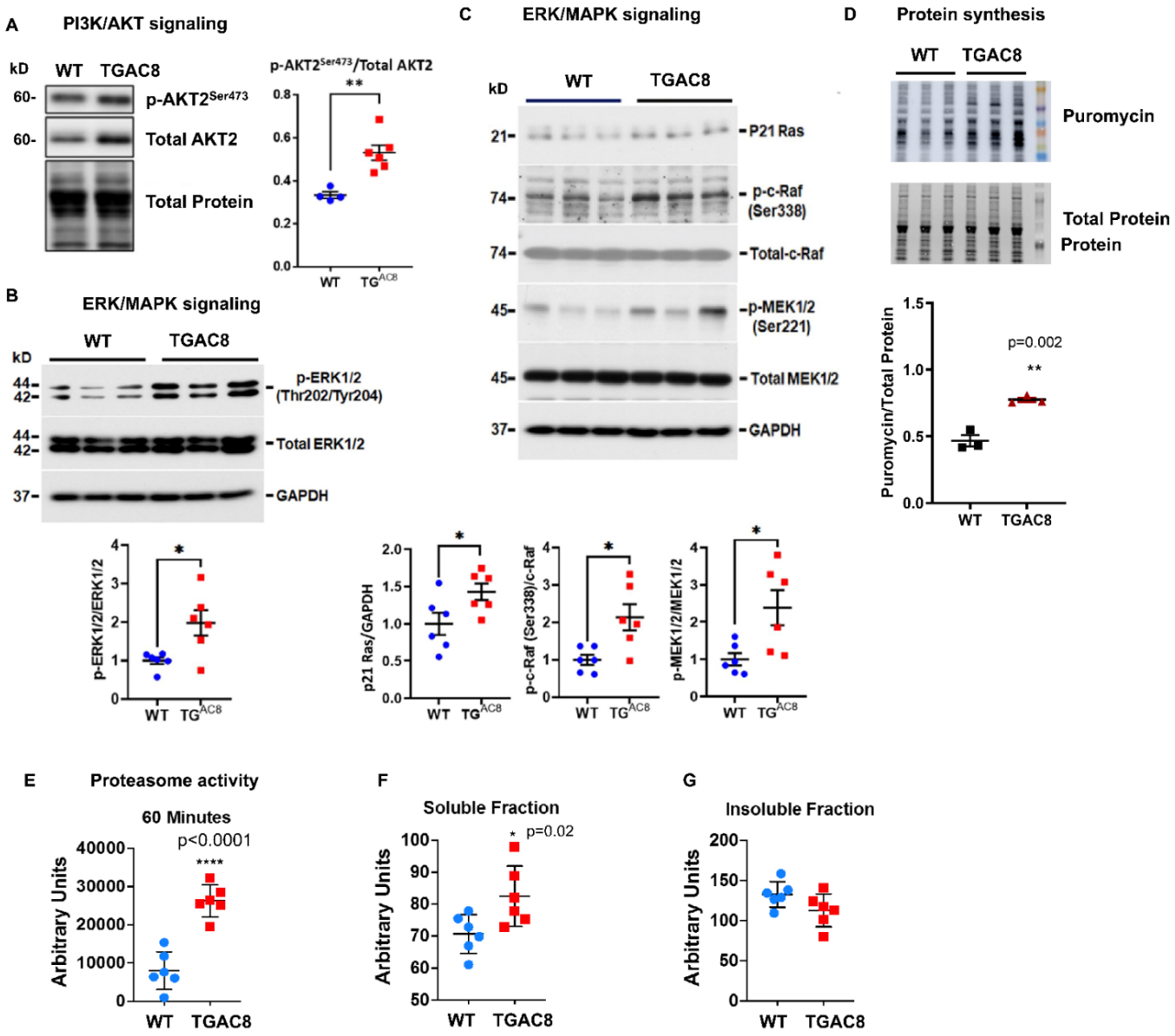

1026

1027

1028

1029 **Figure 7. Analyses of proteins changed discordantly in proteome and phosphoproteome.**

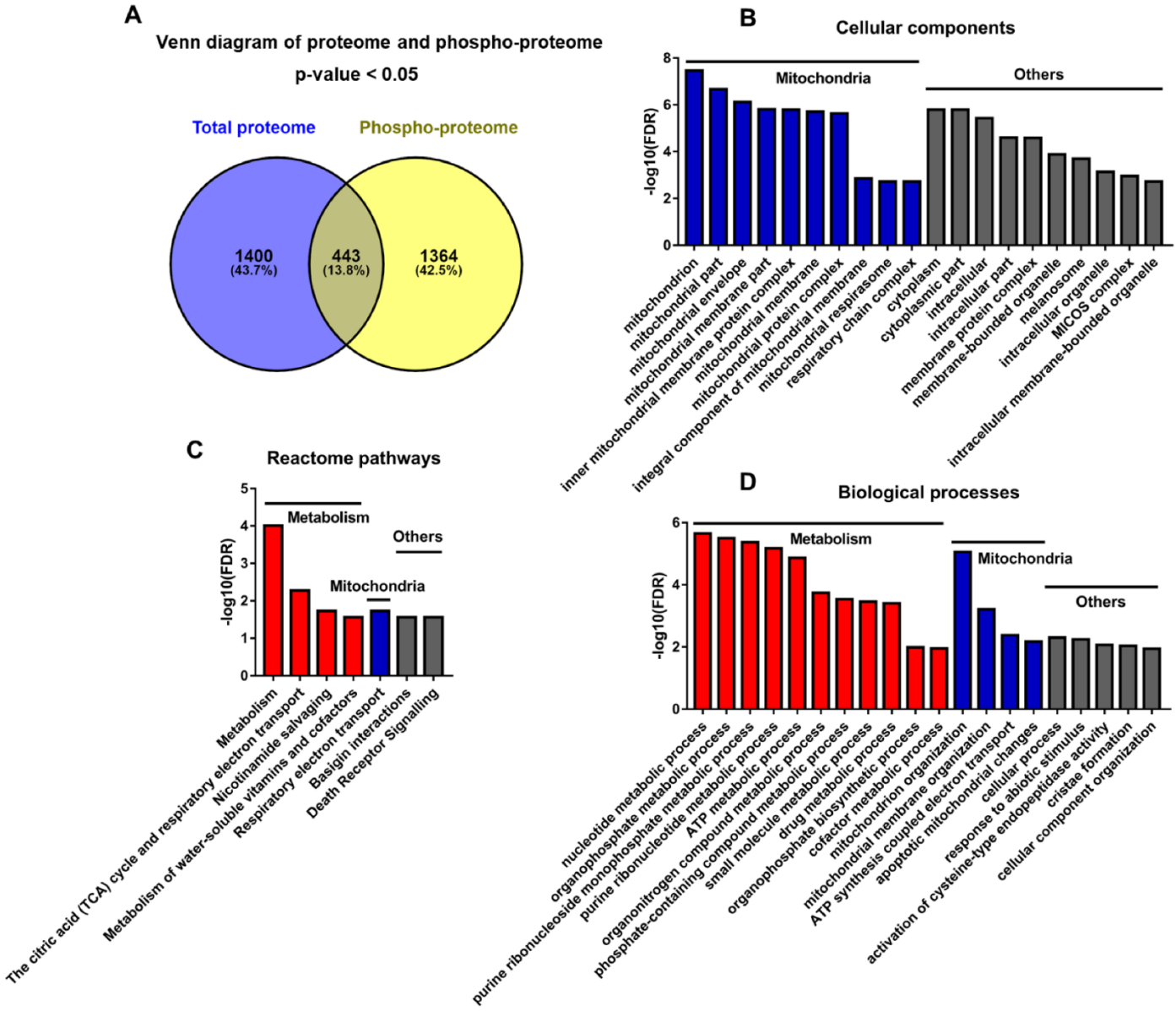

1031

1032

1033

1034

1035 **Figure 8. Deduced schematic of coordination of phosphoproteome with transcriptome and**

1036 **proteome in TGAC8 mouse LV.**

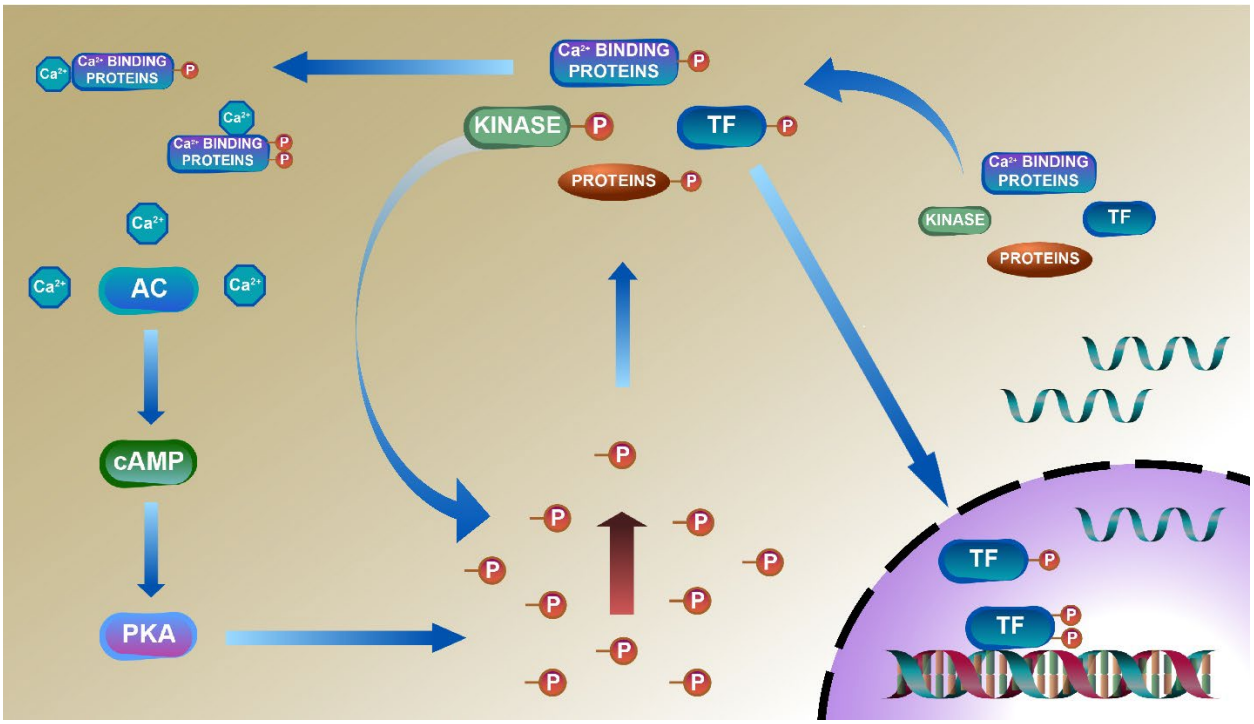

1037

1038

1039

1040

1041

1042

1043

1044

1045 **Appendix-figure 1. A comprehensive circuitry of TGAC8 mouse heart concluded from this**

1046 **phosphoproteome combine with previous transcriptome and proteome.**

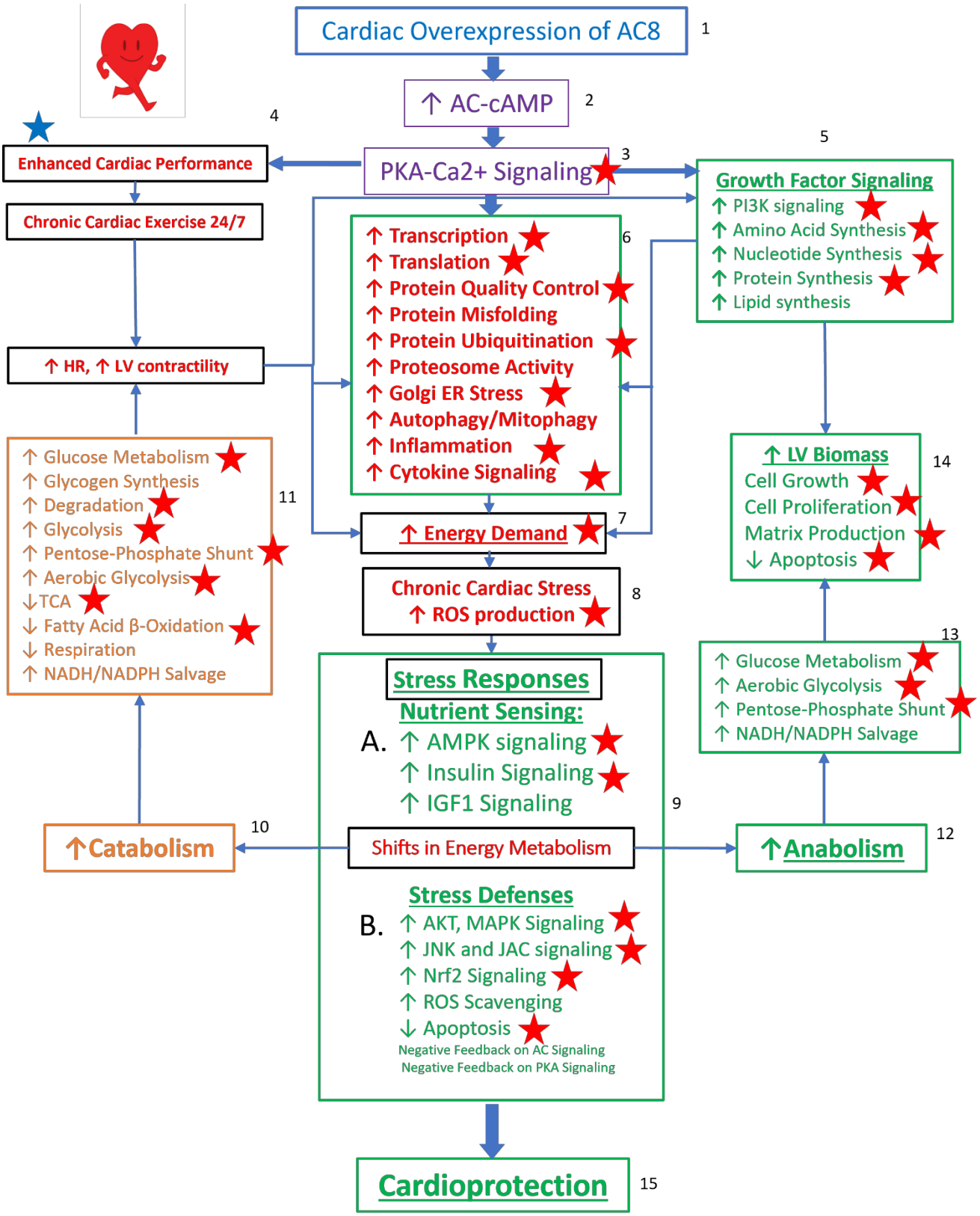
Cardiac Overexpression of AC8
1
↑ AC-cAMP
2
PKA-Ca2+ Signaling
3
4
Enhanced Cardiac Performance
Chronic Cardiac Exercise 24/7
↑ HR, ↑ LV contractility
5
Growth Factor Signaling
↑ PI3K signaling
↑ Amino Acid Synthesis
↑ Nucleotide Synthesis
↑ Protein Synthesis
↑ Lipid synthesis
6
↑ Transcription
↑ Translation
↑ Protein Quality Control
↑ Protein Misfolding
↑ Protein Ubiquitination
↑ Proteosome Activity
↑ Golgi ER Stress
↑ Autophagy/Mitophagy
↑ Inflammation
↑ Cytokine Signaling
7
↑ Energy Demand
8
Chronic Cardiac Stress
↑ ROS production
11
↑ Glucose Metabolism
↑ Glycogen Synthesis
↑ Degradation
↑ Glycolysis
↑ Pentose-Phosphate Shunt
↑ Aerobic Glycolysis
↓TCA
↓ Fatty Acid β-Oxidation
↓ Respiration
↑ NADH/NADPH Salvage
14
↑ LV Biomass
Cell Growth
Cell Proliferation
Matrix Production
↓ Apoptosis
13
↑ Glucose Metabolism
↑ Aerobic Glycolysis
↑ Pentose-Phosphate Shunt
↑ NADH/NADPH Salvage
Stress Responses
Nutrient Sensing:
A.
↑ AMPK signaling
↑ Insulin Signaling
↑ IGF1 Signaling
9
10
↑Catabolism
Shifts in Energy Metabolism
↑Anabolism
12
Stress Defenses
B.
↑ AKT, MAPK Signaling
↑ JNK and JAC signaling
↑ Nrf2 Signaling
↑ ROS Scavenging
↓ Apoptosis
Negative Feedback on AC Signaling
Negative Feedback on PKA Signaling
Cardioprotection
15

1047